IEEE Access
Multidisciplinary : Rapid Review : Open Access Journal

Received February 1, 2022, accepted February 17, 2022, date of publication February 21, 2022, date of current version March 2, 2022.

Digital Object Identifier 10.1109/ACCESS.2022.3153042

Optimal Allocation of Renewable Distributed Generations Using Heuristic Methods to Minimize Annual Energy Losses and Voltage Deviation Index

MIKAIL PURLU AND BELGIN EMRE TURKAY
Department of Electrical Engineering, Istanbul Technical University, 34469 Istanbul, Turkey
Corresponding author: Mikail Purlu (purlu@itu.edu.tr)

ABSTRACT In this paper, two metaheuristic methods, genetic algorithm and particle swarm optimization, are proposed to determine the optimal locations, sizes, and power factors of single and double distributed generation units. In line with the 2050 carbon neutral goal, the aim was to integrate renewable distributed energy sources such as photovoltaic panels and wind turbines into the distribution system with a high penetration level. In contrast to most studies based on constant loads and dispatchable generations, an application considering the seasonal uncertainties of generation and consumption was performed to minimize the annual energy losses and voltage deviations of the distribution network. In addition, dispatchable, controllable and fuel-based conventional resources were allocated to compare the contributions of renewable resources. These seasonal case studies with various constraints were applied to IEEE 33-bus radial distribution network. To verify the feasibility and robustness of the proposed algorithms, case studies for peak loads were created and compared with the literature studies. While all distributed generation sources were operated at both unity and optimum power factor in all case studies, zero power factor and leading power factor scenarios were examined for a peak load only. Photovoltaic applications without energy storage technologies have not been efficient because of the uneven daily distribution of solar irradiance, especially insufficient irradiation in the evening and excessive irradiation at noon. However, wind energy applications are more reliable and feasible, because the wind speed distribution is relatively more uniform than that of solar irradiation, both seasonally and daily. In all cases, operating distributed generation sources at the optimal power factor provided better results than those operating at unity power factor. Consequently, wind turbines operating at optimal power factors have been found to contribute better than photovoltaic systems, and are almost as good as conventional sources with controllable power output. While both proposed algorithms yielded better results than those in the literature, particle swarm optimization was better than genetic algorithm in terms of providing the best solution, faster convergence, and shorter running time.

INDEX TERMS Distributed power generation, genetic algorithm, heuristic algorithms, optimization methods, particle swarm optimization, photovoltaic systems, power system planning, renewable energy sources, solar energy, wind energy.

NOMENCLATURE

A. ABBREVIATIONS

The abbreviations used throughout this study are as follows.

AM	Analytical method
ALOA	Ant lion optimization algorithm
BA	Bat algorithm
CS	Conventional source
CSFS	Chaotic stochastic fractal search
DAPSO	Dynamic adaptation of PSO
DG	Distributed generation
DS	Distribution system
GA	Genetic algorithm
GSA	Gravitational search algorithm
HHO	Harris hawks optimization
HPSO	Hybrid PSO
HSA	Harmony search algorithm

The associate editor coordinating the review of this manuscript and approving it for publication was Xujie Li.

opf	Optimum power factor
upf	Unity power factor
pf	Power factor
pl	Penetration level
PPA	Plant propagation algorithm
PSO	Particle swarm optimization
PV	Photovoltaic
RDN	Radial distribution network
RES	Renewable energy source
SA	Simulated annealing
SS	Substation
SSA	Salp swarm algorithm
TSA	Tabu search algorithm
VDI	Voltage deviation index
VSI	Voltage stability index
WCA	Water cycle algorithm
WT	Wind turbine

B. SYMBOLS

The symbols used in this paper are described below.

AEL_a	Annual active energy loss
AEL_r	Annual reactive energy loss
c_1, c_2	Acceleration parameters of PSO
CEL_a	Contribution to active energy loss
CPL	Contribution to active power loss
CQL	Contribution to reactive power loss
CU_{min}	Contribution to minimum voltage
EL_a	Active energy loss
EL_r	Reactive energy loss
I_i^{max}	Maximum current capacity of i^{th} branch
I_i^t	Current of i^{th} branch at any time
$Gbest^k$	Best solution of all particles at iteration k
k	Current iteration value
k_{max}	The number of maximum iterations
L_{DG}	Location of DG
n	Number of particles
N	Number of DGs
N_{bus}	Number of buses in the DS
N_{line}	Number of branches in the DS
$Pbest_i^k$	Best solution of i^{th} particle at iteration k
P_D	Total active power demand
$P_{DG,i}$	Active power generation of i^{th} DG
$P_{DG,i}^{max}$	Maximum active power capacity of DG_i
$P_{DG,i}^{min}$	Minimum active power capacity of DG_i
P_G	Active power injected by substation
P_L^t	Total active power loss at any time
$P_L^{no\ DG}$	Active power loss before DG integration
$P_L^{with\ DG}$	Active power loss after DG integration
r_1, r_2	Random numbers between 0 and 1
Q_D	Total reactive power demand
$Q_{DG,i}$	Reactive power generation of DG_i
$Q_{DG,i}^{max}$	Maximum reactive power capacity of DG_i
$Q_{DG,i}^{min}$	Minimum reactive power capacity of DG_i
Q_G	Reactive power injected by substation
Q_L^t	Total reactive power loss at any time
$Q_L^{no\ DG}$	Reactive power loss before DG integration
$Q_L^{with\ DG}$	Reactive power loss after DG integration
R_i	Resistance of i^{th} line
S_{DG}	Apparent power of DG
S_{load}	Apparent power of the loads
U_i	Voltage magnitude of i^{th} bus
$U_i^{no\ DG}$	Voltage magnitude of i^{th} bus before DG
$U_i^{with\ DG}$	Voltage magnitude of i^{th} bus after DG
U_{max}	Maximum voltage limit of the system
U_{min}	Minimum voltage limit of the system
$U_{min}^{no\ DG}$	The worst voltage before DG installation
$U_{min}^{with\ DG}$	The worst voltage after DG installation
U_n	Nominal voltage value
$VDI^{no\ DG}$	VDI before DG integration
$VDI^{with\ DG}$	VDI after DG integration
V_i	Velocity of i^{th} particle
X_i	Reactance of i^{th} line
χ_i	Position of i^{th} individual
w_1	Weighting coefficient of active loss
w_2	Weighting coefficient of reactive loss
w_3	Weighting coefficient of VDI
ω	Inertia weight
ω_{max}	Maximum (initial) weight
ω_{min}	Minimum (final) weight

I. INTRODUCTION

The increase in the demand for electrical energy day by day and the transmission of energy over long distribution feeders cause great power losses and voltage drop problems. These problems negatively affect both the performance of the power system and reliability of the customers' power supply. [1].

Because of its numerous positive effects on distribution system (DS) planning and operation, modern electricity systems or smart grids focus on distributed (dispersed, decentralized) generation (DG) rather than centralized generation.

DG is defined as small-scale power generation close to the connection point of consumers [2]. Generation capacity of DG is defined by the Electric Power Research Institute between a few kW and 50 MW [3].

The load flow is from generation stations to consumption areas in the DS only with centralized generation, while it is bidirectional in the DS with DGs. If this topological change is not well planned, it may cause deterioration of various power quality parameters, protection problems, and insufficient or excessive electricity generation. When DGs are optimally allocated, all relevant parameters are improved, and power losses and carbon emissions are also reduced.

The benefits of optimum DG planning can be categorized as follows [4].

- **Technical benefits:**
  - Enhanced voltage support by improving voltage profile
  - Reducing the system losses by integrating DG into strategic positions

  - Enhanced system reliability and system security and power quality
  - Increasing the overall electric energy efficiency due to diversification of resources
  - Power supply autonomy of rural or isolated areas
- **Economic benefits:**
  - Lower operating costs due to peak shaving
  - Reduced fuel costs due to increased overall efficiency
  - Lowering operation and maintenance costs
  - Deferment of investment costs for upgrade of facilities
  - An indirect monetary benefit by reduce healthcare costs due to improved environment
- **Environmental benefits:**
  - Reducing the investment risks
  - Reducing emissions thanks to renewable DGs
  - Reducing global warming by encouraging use of renewable energy

As pressure mounts on climate action, the more use of renewable energy sources (RESs) instead of fuel-based conventional sources (CSs) has started to increase even more. Thanks to advances in renewable technologies and cheaper costs, the green revolution to build an energy system with net-zero greenhouse gas emissions is happening faster than previously thought.

A. DG TYPES, CAPACITIES AND TECHNOLOGIES

DGs are divided into four groups according to their generation or consumption status of active and reactive power, which depend on their power factor (pf) [5].

Type I: DGs, such as photovoltaic (PV) systems, micro turbines and fuel cells, operate at unity pf (upf) and generate only active power.

Type II: DGs, such as synchronous compensators, operate at zero pf and generate only reactive power.

Type III: DGs, such as synchronous generator and wind turbine (WT), operate at lagging pf and generate both active and reactive power.

Type IV: DGs, such as induction generators, operate at leading pf and generate active power and consume reactive power.

Based on the current IEEE 1547 standard, DGs can be integrated into the grid at the desired pf with help of the proper invertors or convertors [6].

DGs are classified according to their generation capacity as follows [3].

Micro DG: between 1 W and 5 kW;
Small DG: between 5 kW and 5 MW;
Medium DG: between 5 MW and 50 MW;
Large DG: between 50 MW and 300 MW.

Distributed energy resources can be categorized according to their generation technologies as follows [7].

- **DG technologies**
  - ○ Conventional generators
    - ☐ Diesel
    - ☐ Gas
      - Micro-turbines
      - Combustion turbines
  - ○ Non-conventional generators
    - ☐ Electrochemical Devices
      - Fuel Cells
    - ☐ Renewable DGs
      - Photovoltaics
      - Wind (Land-based and off-shore)
      - Biomass
      - Solar thermal
      - Geothermal
      - Small hydro turbines
- **Energy storage technologies**
  - Battery energy storage systems
  - Flywheel
  - Superconducting magnetic energy storage
  - Compressed air energy storage
  - Pumped storage

B. LITERATURE REVIEW

The general objective functions of optimal DG placement problems are to reduce active losses and investment or operating costs, and to improving voltage profile of the power systems. In the literature, analytical methods, heuristic methods and hybrid of both methods have been used to find optimum location and size of DG for constant load (peak load) and time varying loads.

In [2], various particle swarm optimization (PSO) and differential evolutionary techniques were proposed for the placement of 1, 2 and 3 DGs in Type-I with minimum output power in order to minimize active losses on IEEE 33 and 69-bus radial distribution networks (RDNs). The best results of their study were obtained with dynamic adaptation of PSO (DAPSO).

A heuristic hybrid method of Harris hawks optimization (HHO) and PSO [4] was used to minimize active power loss, annual active energy loss, voltage deviation index (VDI) and improve voltage stability index (VSI) by placing 1, 2 and 3 PVs and WTs on IEEE 33-bus, IEEE 69-bus and 94-bus Portuguese real RDNs.

In [8], genetic algorithm (GA) was proposed to optimal placement of 1-4 DGs in Type-I for minimizing total active losses on IEEE 33 and 69-bus RDNs.

The authors in [9] determined the optimum location of single DG in Type I after finding the optimum DG size with PSO for all buses between 2 and 26 of the 26-bus practical RDN located in Thailand.

Single, double and triple DGs in Type-I were allocated to IEEE 33 and 69-bus RDNs for minimizing active loss and improving voltage profile by using harmony search algorithm (HSA) with a differential operator [10].

Gravitational search algorithm (GSA) was proposed for optimum integration of single and double DGs in Type I on

13-bus RDN in order to reduce active losses, and improve voltage deviation and voltage harmonic distortion [11].

In [12], a hybrid method of GSA and phasor PSO was proposed to find the optimum location and size of 1, 2 and 3 PVs to reduce active losses and improve voltage stability on 94-bus practical RDN located in Portuguese.

An improved PSO algorithm [13] was proposed to reduce active losses on IEEE 34-bus RDN by placing only single DG in type I with a maximum DG penetration limit of 41.15%.

The authors in [14] suggested the plant propagation algorithm (PPA) to maximize active loss reduction and minimum bus voltage by integrating 1-4 DGs in Type-I into IEEE 33 and 69-bus RDNs.

Simulated annealing (SA) [15] for 1-4 DGs placement in Type-I and bat algorithm (BA) [16] for 3 solar based DGs placement in Type-I were proposed to reduce active power loss on IEEE 33-bus RDN.

In [17], chaotic stochastic fractal search (CSFS) method for 1-3 DGs placement in Type-I on IEEE 33, 69 and 118-bus RDNs were studied to minimize active losses.

The authors in [18] used two algorithms such as student psychology-based optimization algorithm and HHO algorithm to solve optimal DG placement problem with cost analysis, and tested on IEEE 33 and 69-bus, and Brazil 136-bus RDNs.

An analytic method (AM) [19] for optimal 1-3 DGs placement in Type-III was introduced to reduce active power loss on IEEE 15 and 33-bus RDNs.

In [20], hybrid PSO (HPSO) was proposed to maximize the loadability and minimize active loss by installing 1-3 DGs in Type-III to IEEE 16, 33 and 69-bus RDNs.

For 1-5 DGs placement in Type-I&III, chimp optimization algorithm [21] was applied to reduce active power loss on IEEE 33, 69 and 119-bus RDNs.

Improved decomposition based evolutionary algorithm [22] for 1-7 DGs in Type I&III were tested on IEEE 33, 69 and 119-bus RDN to minimize active power loss and voltage deviation and maximize VSI.

Water cycle algorithm (WCA) [23] for optimal 3 DGs placement in Type-I&III with network reconfiguration was introduced and tested on IEEE 33 and 69-bus RDNs.

Single and double renewable DGs such as PV (Type-I) and WT (Type-III) placement problems were solved by ant lion optimization algorithm (ALOA) on IEEE 33 and 69-bus RDNs [24].

Salp swarm algorithm (SSA) [25] was used to optimize wind DG sitting in Type-I for time varying voltage dependent load models on IEEE 33 and 69-bus RDNs.

In [26], to minimize daily power losses on the modified IEEE 14-bus, solar DG allocation in Type-I was provided by using GA and PSO.

Hybrid of greedy randomized adaptive search and tabu search algorithm (TSA) were used to maximize penetration level (pl) of both renewable DGs and electric vehicles and tested on IEEE 33, 83 and 135-bus RDNs [27].

Multi objective approach of symbiosis organism search and neural network algorithm was introduced for optimum allocation of 3 DGs in Type-I&III and capacitor banks on 33 and 69-bus RDNs [28].

The authors in [29] proposed rider optimization algorithm to optimum allocation of PV (Type-I), WT (Type-III), biomass and battery energy storage systems on IEEE 33 and 69-bus RDNs for daily profiles of load and generation.

In [30], political optimization algorithm was proposed to place optimal multiple DGs and shunt capacitors for minimizing power losses and improving voltage profile and VSI of the standard IEEE 33-bus RDN in 24 hours.

Modified rainfall optimization [31] for DG allocation and network reconfiguration was proposed to minimize active power loss and operating cost, and enhance voltage profile and VSI on the IEEE test systems, 33-bus and 69-bus.

Artificial ecosystem optimization [32] was used to lessen total active power loss of the practical 59-bus Cairo DS in Egypt via capacitor and DG allocation, and network reconfiguration. Also, the methods such as jellyfish search optimization, supply demand optimization, crow search optimization, PSO, grey wolf optimization and whale optimization algorithm were used to compare with the proposed algorithm.

To ensure optimal allocation of DGs and electric vehicles on IEEE 33-bus RDN in 24 hours, enhanced grasshopper optimization algorithm was proposed to minimize power losses and improve voltage profile [33].

In [34], the authors have proposed machine learning methods to estimate the DG size and its effects on DS. The proposed methods such as Linear Regression, Artificial Neural Networks, Support Vector Regression, K-Nearest Neighbor and Decision Tree were applied on IEEE 12, 33 and 69-bus standard test systems. They show that estimation methodologies are effective on DG allocation problems and they can be alternative to the load flow-based techniques, which takes a long time.

Most studies in the literature have been carried out with type-I and type-III DGs assuming that the load and DG output profile are either constant or mostly show a 24-hour average change. However, in practice generation profiles, especially for RESs, and consumption profiles are more complex and vary more frequently than 24 hours in a year.

In this study, all DG types and seasonal uncertainties consisting of a total of 96 hours, with a 24-hour average from each season, were considered to determine optimal locations, sizes and pf of both fuel-based and renewable sources by GA and PSO.

C. NOVELITY AND CONTRIBUTIONS

In this paper, the authors propose following contributions:

- Applying of all DG types, especially type-IV, to the test system to determine the most suitable DG operating condition and their effects in various aspects.
- Considering the seasonal uncertainty of load and generation profiles with a total of 96 hours.

- In all case studies, obtaining the best solutions via two proposed heuristic algorithms, GA and PSO.
- Usage of renewable DG with a high penetration in line with the net-zero carbon target and performance comparison with fuel-based sources.
- Providing diversity and comparison opportunities by using both PV and WT as renewable energy sources.
- Operation of all sources at both upf and optimal pf (opf) to determine the most appropriate pf and to demonstrate its effects.
- Operation of PVs not only at ups as in the literature studies, but also at opf in accordance with the current IEEE 1457 standard as a novel contribution.

D. PAPER ORGANIZATION

The rest of this paper is arranged as follows. In Section II, the mathematical expressions of the optimal DG placement problems are introduced. In Section III, the proposed algorithms are defined and their application steps are described. In Section IV, the case studies and simulation results are presented. The results are discussed in Section V. Finally, the conclusion part is provided in Section VI.

II. PROBLEM FORMULATIONS

In electrical power systems, active and reactive power losses are calculated as follows [25].

$$P_L^t = \sum\nolimits_{i=1}^{N_{line}} \left\{ \left(I_i^t\right)^2 \times R_i \right\} \tag{1}$$

$$Q_L^t = \sum\nolimits_{i=1}^{N_{line}} \left\{ \left(I_i^t\right)^2 \times X_i \right\} \tag{2}$$

where, P_L^t is total active power loss in kW, Q_L^t is total reactive power loss in kVAr, and I_i^t is the current in kA of i^{th} line (branch) at time t; N_{line} is the number of lines; R_i and X_i are the resistance and reactance of i^{th} line in Ω.

Active and reactive energy losses during Δt are calculated using (3) and (4), respectively [1].

$$EL_a = P_L^{\Delta t} \times \Delta t \tag{3}$$

$$EL_r = Q_L^{\Delta t} \times \Delta t \tag{4}$$

where, EL_a is active energy loss in kWh and EL_r is reactive energy loss in kVArh.

Considering the hourly load demand ($\Delta t = 1hour$), the total annual active and reactive energy losses are calculated as follows.

$$AEL_a = \sum\nolimits_{t=1}^{8760} P_L^t \tag{5}$$

$$AEL_r = \sum\nolimits_{t=1}^{8760} Q_L^t \tag{6}$$

where, AEL_a is total annual active energy loss in kWh, and AEL_r is total annual reactive energy loss in kVArh.

For the seasonal average load profile, the annual energy losses can be calculated as follows.

$$AEL_a = \frac{365}{4} \sum\nolimits_{S=1}^{4} \left\{ \sum\nolimits_{t=1}^{24} P_L^{t,s} \right\} \tag{7}$$

$$AEL_r = \frac{365}{4} \sum\nolimits_{S=1}^{4} \left\{ \sum\nolimits_{t=1}^{24} Q_L^{t,s} \right\} \tag{8}$$

where, s represents the seasons such as winter, spring, summer and autumn for values 1, 2, 3 and 4, respectively.

The voltage deviation index (VDI), which shows the closeness of the bus voltages to the nominal voltage value, is calculated as follows [35], [36].

$$VDI = \sum\nolimits_{t=1}^{T} \sum\nolimits_{i=1}^{N_{bus}} \left(U_n - U_{i,t}\right)^2 \tag{9}$$

where, U_n is nominal voltage magnitude value and it equals to 1 pu; T is number of hours; N_{bus} is number of buses; $U_{i,t}$ is voltage of i^{th} bus at time t.

A. OBJECTIVE FUNCTIONS

The typical optimal DG allocation problems aim to maximize positive effects and minimize negative effects on the power systems. In this paper, there are two objective functions: multi-objective function to minimize active and reactive power losses and to maximize voltage profile improvement, and single-objective function to minimize annual active energy loss. These multi and single-objective functions are as follows.

$$min\ F_1 = w_1 \frac{P_L^{with\ DG}}{P_L^{no\ DG}} + w_2 \frac{Q_L^{with\ DG}}{Q_L^{no\ DG}} + w_3 \frac{VDI^{with\ DG}}{VDI^{no\ DG}} \tag{10}$$

$$min\ F_2 = AEL_a \tag{11}$$

where, w_1, w_2 and w_3 are weighting coefficients of active loss, reactive loss and VDI, respectively; $\mathrm{P_L^{with\ DG}}$ and $\mathrm{Q_L^{with\ DG}}$ are active and reactive power losses after DG integration; $\mathrm{P_L^{no\ DG}}$ and $\mathrm{Q_L^{no\ DG}}$ are active and reactive power loses before DG integration; $\mathrm{VDI^{with\ DG}}$ and $VDI^{no\ DG}$ are voltage deviation indexes after and before DG integration.

B. CONSTRAINTS

1) POWER BALANCE CONSTRAINTS

In power systems, the sum of all generated powers equal to the sum of demand powers and power losses. It is expressed as power balance and formulated as follows [37].

$$P_G + \sum\nolimits_{i=1}^{N} P_{DG,i} = P_d + P_L \tag{12}$$

$$Q_G + \sum\nolimits_{i=1}^{N} Q_{DG,i} = Q_d + Q_L \tag{13}$$

where, N is number of DGs; P_G and Q_G are active and reactive power injected by main substation; $P_{DG,i}$ and $Q_{DG,i}$ are active and reactive power generated by i^{th} DG; P_d and Q_d are total active and reactive demand powers of the system.

2) VOLTAGE CONSTRAINTS

Two voltage constraints used in this study are represent by (14) and (15) for voltage constraint-1 and 2, respectively.

$$U_i^{no\ DG} \leq U_i^{with\ DG} \tag{14}$$

$$U_{min} \leq |U_i| \leq U_{max} \tag{15}$$

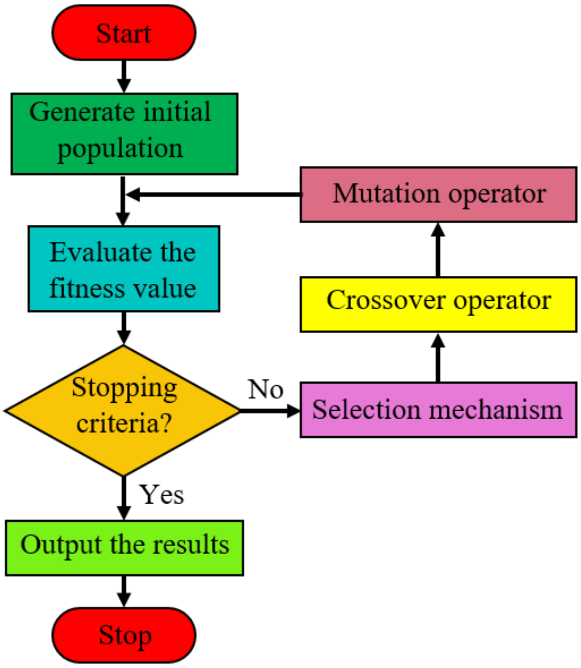

FIGURE 1. The simplified flowchart of GA [47], [48].

TABLE 1. Parameter settings for GA.

Parameter	Value
Control variables	Size, location and pf of DG
Population size	20
Crossover rate	0.6
Mutation rate	0.05
Elitism rate	0.05
Maximum iteration number	100

where, $\mathrm{U}_i^{\text{no DG}}$ and $\mathrm{U}_i^{\text{with DG}}$ are voltage value of i^{th} bus before and after DG integration, respectively; U_{min} and U_{max} are minimum and maximum bus voltage limits and their values are 0.95 and 1.05 pu, respectively.

Voltage constraint-1 means that any bus voltage after DG integration cannot get worse than before DG placement. In voltage constraints-2, the voltage values of all buses after DG integration must be between 0.95 and 1.05 pu [2], [13], [18].

3) DG CONSTRAINTS

Power generation units have minimum and maximum generation limits and they are represented as follows [38].

$$P_{DG,i}^{min} \leq P_{DG,i} \leq P_{DG,i}^{max} \tag{16}$$

$$Q_{DG,i}^{min} \leq Q_{DG,i} \leq Q_{DG,i}^{max} \tag{17}$$

DG locations cannot be at the same bus or slack bus and these constraints are defined as follows [17], [20].

$$2 \leq L_{DG_i} \neq L_{DG_j} \leq N_{bus} \tag{18}$$

where, L_{DGi} and L_{DGj} represent the positions of i^{th} and j^{th} DG.

In addition to (16), (17) and (18), seasonal uncertainties of renewable energy sources should be considered.

TABLE 2. Parameter settings for PSO.

Parameter	Value
Control variables	Size, location and pf of DG
Particle size	20
Acceleration coefficient ($c_1 = c_2$)	2
Inertia weights (ω_{min} and ω_{max})	0.1 and 0.9
Maximum iteration number	100

4) TERMAL CONSTRAINT

The current of i^{th} line at any time, I_i^t, must be less than the maximum current capacity of this branch, I_i^{max}, and it represents as follows [39].

$$I_i^t \leq I_i^{max} \tag{19}$$

5) OTHER CONSTRAINTS

Any index of the power system or power quality parameter such as active loss, reactive loss, minimum voltage value and VDI after DG installation cannot get worse than before DG integration. These constraints are shown as follows.

$$P_L^{after\ DG} \leq P_L^{before\ DG} \tag{20}$$

$$Q_L^{after\ DG} \leq Q_L^{before\ DG} \tag{21}$$

$$U_{min}^{beforDG} \leq U_{min}^{after\ DG} \tag{22}$$

$$VDI^{after\ DG} \leq VDI^{before\ DG} \tag{23}$$

C. EVALUATION METRICS

In order to evaluate the contribution of DG placement to the grid, contribution indexes in percentage can be calculated as follows.

$$CPL = \frac{P_L^{no\ DG} - P_L^{with\ DG}}{P_L^{no\ DG}} \times 100\% \tag{24}$$

$$CQL = \frac{Q_L^{no\ DG} - Q_L^{with\ DG}}{Q_L^{no\ DG}} \times 100\% \tag{25}$$

$$CU_{min} = \frac{U_{min}^{with\ DG} - U_{min}^{no\ DG}}{U_{min}^{no\ DG}} \times 100\% \tag{26}$$

$$CEL_a = \frac{EL_a^{no\ DG} - EL_a^{with\ DG}}{EL_a^{no\ DG}} \times 100\% \tag{27}$$

where, CPL and CQL are contribution to active and reactive power losses, respectively [20]; CU_{min} is contribution to minimum voltage value; CEL_a is contribution to annual active energy loss.

Penetration level of DG is calculated as follows [20], [25].

$$\%pl = \frac{S_{DG}}{S_{load}} \times 100 \tag{28}$$

where, S_{DG} is apparent power of DG; S_{load} is apparent power of the loads in the systems.

III. OVERVIEW OF THE PROPOSED METHODS

Heuristic algorithms can provide near-optimal solutions for large-scale optimization problems within acceptable time

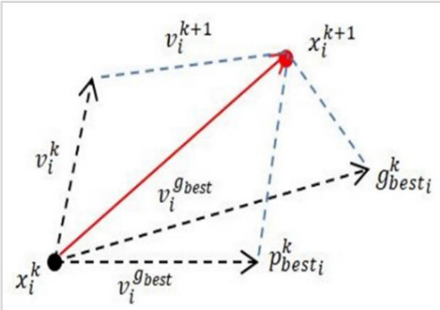

FIGURE 2. The vectoral path for velocity and position updates followed by each particle in PSO algorithm [54], [55].

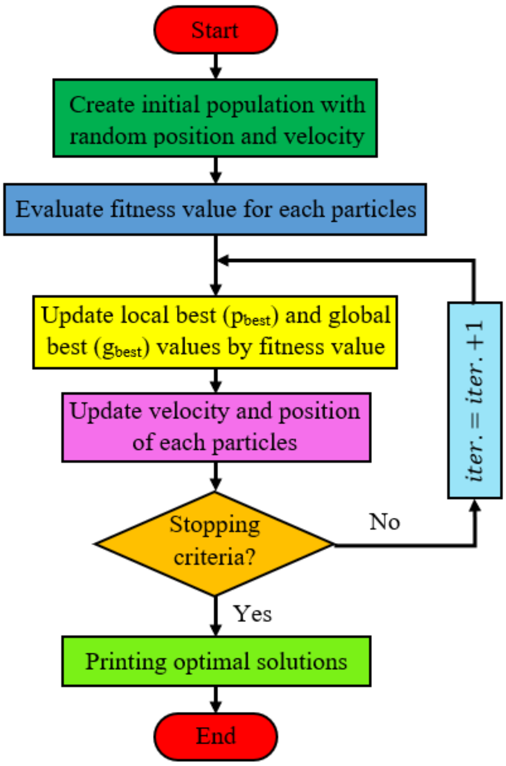

FIGURE 3. The simplified flowchart of PSO [56].

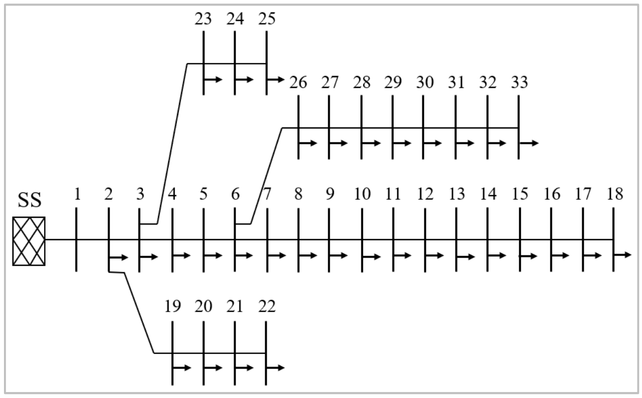

FIGURE 4. Single line diagram of the standard IEEE 33-bus RDN [57].

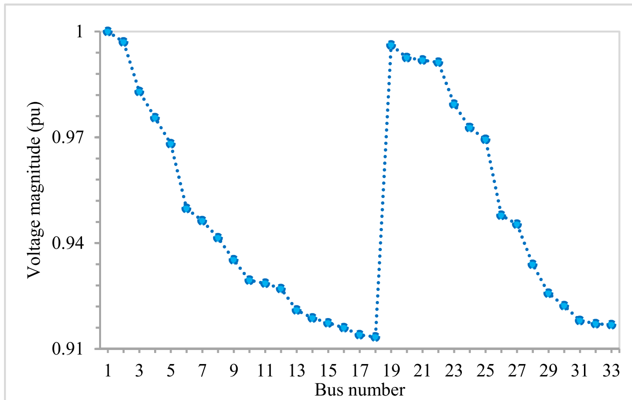

FIGURE 5. Bus voltages of the system at base case.

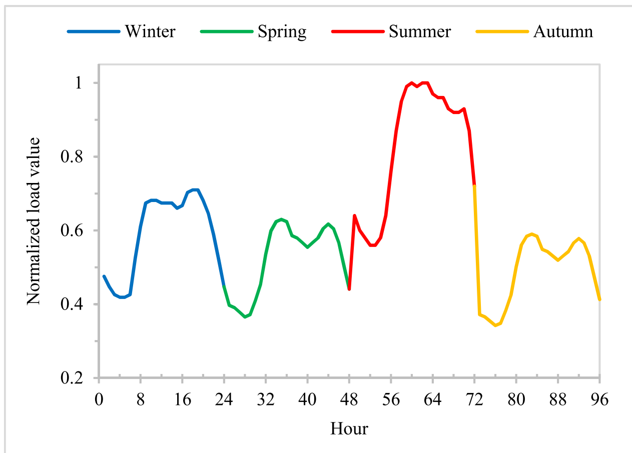

FIGURE 6. Seasonal load profile [34].

limits. These algorithms are generally classified into six different groups: biology-based, physics-based, herd-based, social-based, music-based and chemistry-based. Swarm intelligence-based optimization algorithms have been developed by examining the movements of swarms such as birds, fish, cats and bees [40].

Examples of heuristic algorithms include GA, PSO, HSO, PPA, BA, SA, WCA, ALOA, SSA, TSA, ant colony optimization, artificial bee colony, differential evaluation algorithm, grey wolf optimization, and whale optimization algorithm.

In this study, two heuristic algorithms, GA and PSO, were proposed to solve the optimal DG placement problem.

A. GENETIC ALGORITHM

Inspired by Darwin's theory of evolution, GA was first introduced by John Henry Holland in 1975 [41], and later developed by David Goldberg in 1989 [42]. The birth, reproduction, and extinction of living organisms were artificially imitated in the GA.

First, a random initial population is created and the fitness value of each individual is calculated. If the stopping criteria are met, the search process is stopped. Otherwise, new individuals are produced by genetic operators [43]. Genetic operators are reproduction, crossover, recombination, and mutation [44]. The elitism operator is used to protect better individuals from older generations [45]. A certain time,

TABLE 3. Outputs of optimum solutions for case 1A.

DG parameters		Cases	TYPE II GA	TYPE II PSO	TYPE IV GA	TYPE IV PSO
1DG	DG1	L	30	30	29	29
		pf	0	0	0.9	0.9
		kW	0	0	675.3	733.5
		kVAr	1038.2	1069.7	-327.0	-305.2
		kVA	1038.2	1069.7	750.3	815.0
		pl (%)	23.76	24.48	17.17	18.65
2DG	DG1 of 2DG	L	30	30	29	29
		kVA	791.8	933.0	432.7	584.4
		pf	0	0	0.9	0.9
		kW	0	0	389.4	526.0
		kVAr	791.8	933.0	-188.6	-254.7
	DG2 of 2DG	L	12	13	13	13
		kVA	532	300	404.7	351.6
		pf	0	0	0.9	0.9
		kW	0	0	364.2	316.4
		kVAr	532.1	299.8	-176.4	-153.3
	Total of 2DG	kW	0	0	753.7	842.4
		kVAr	1323.9	1232.8	-365.0	-408.0
		kVA	1323.9	1232.8	837.4	936.0
		pl (%)	30.30	28.21	19.17	21.42

TABLE 4. Outputs of optimum solutions for case 1B.

DG parameters		Cases	TYPE I GA	TYPE I PSO	TYPE III GA	TYPE III PSO
1DG	DG1	L	6	6	6	6
		pf	1	1	0.84	0.83
		kW	2685.3	2679.8	2536.6	2635.7
		kVAr	0	0	1638.5	1771.2
		kVA	2685.3	2679.8	3019.8	3175.6
		pl (%)	61.46	61.33	69.11	72.68
2DG	DG1 of 2DG	L	30	29	32	30
		kVA	169.0	97.8	657.8	557.3
		pf	1	1	0.7141	0.44
		kW	169.0	97.8	469.7	245.2
		kVAr	0	0	460.5	500.5
	DG2 of 2DG	L	6	6	6	6
		kVA	2553	2584	2522	2690
		pf	1	1	0.8564	0.88
		kW	2552.5	2584.4	2160.2	2367.2
		kVAr	0	0	1302.4	1277.7
	Total of 2DG	kW	2721.5	2682.2	2629.9	2612.5
		kVAr	0.0	0.0	1762.9	1778.2
		kVA	2721.5	2682.2	3166.1	3160.2
		pl (%)	62.29	61.39	72.46	72.33

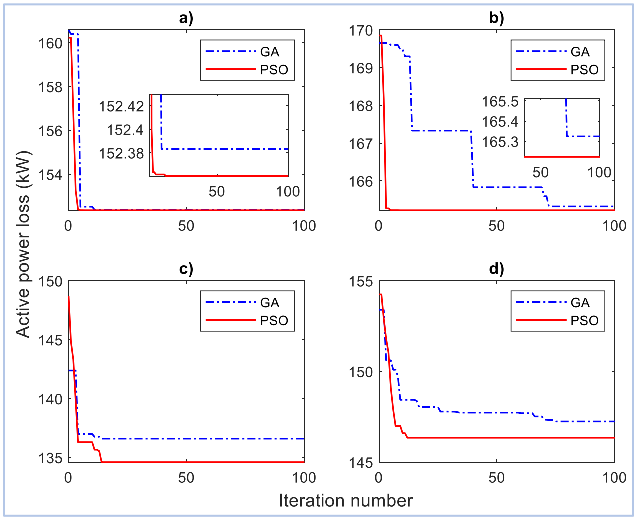

FIGURE 7. Convergence characteristics of the proposed algorithms in case 1A for a) 1 DG placement of Type II; b) 1DG placement of Type IV; c) 2 DGs placement of Type II; d) 2DGs placement of Type IV.

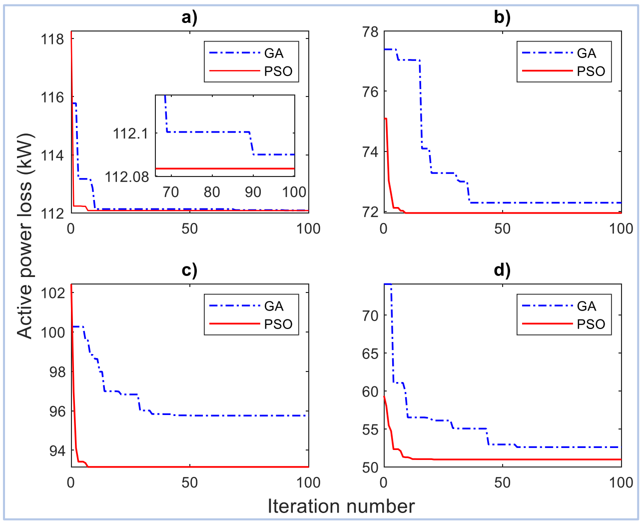

FIGURE 8. Convergence characteristics of the proposed algorithms in case 1B for a) 1 DG placement of Type I; b) 1 DG placement of Type III; c) 2 DGs placement of Type I; d) 2 DGs placement of Type III.

consecutive iterations, and reaching a specific response or maximum iteration number can be selected as algorithm stopping criteria.

The implementation steps of GA are generally as follows [46]:

Step 1: A random initial population is generated and the iteration counter is set to zero.

Step 2: When the chromosomes that satisfy the constraints of the problem reach the desired number, the next stage is passed.

Step 3: Fitness values are calculated for each chromosome. Elitism is performed by maintaining chromosomes with the best fitness value.

Step 4: The crossover operation is applied to individuals selected according to the fitness value among the non-elite individuals.

Step 5: Some of the individuals selected from the new population are randomly mutated, and new individuals are created by randomly selecting some of them without mutation.

Step 6: Some new individuals are randomly mutated and new individuals are generated.

Step 7: A part of the population is preserved without mutation.

Step 8: The fitness values of all created populations are calculated and these processes are repeated until the stopping criteria are satisfied.

Step 9: When the stopping criteria are satisfied, the algorithm is terminated and the optimum results are printed.

A simplified flowchart of the GA is shown in Fig. 1 [47], [48], and the parameter values suitable for the GA developed in this study are listed in Table 1.

TABLE 5. Outputs of optimum solutions for case 1C.

DG parameters		Cases	TYPE I GA	TYPE I PSO	TYPE III GA	TYPE III PSO
1DG	DG1	L	6	6	6	6
		pf	1	1	0.84	0.83
		kW	3117.9	3125.0	3025.1	2888.1
		kVAr	0	0	1954.0	1940.8
		kVA	3117.9	3125.0	3601.3	3479.7
		pl (%)	71.36	71.52	82.42	79.64
2DG	DG1 of 2DG	L	29	29	32	30
		kVA	155.2	43.7	745.4	523.4
		pf	1	1	0.65	0.47
		kW	155.2	43.7	486.6	246.0
		kVAr	0	0	564.6	462.0
	DG2 of 2DG	L	6	6	6	6
		kVA	2956	3000	2681	2943
		pf	1	1	0.87	0.88
		kW	2955.7	2999.8	2332.6	2590.3
		kVAr	0	0	1321.9	1398.1
	Total of 2DG	kW	3110.9	3043.5	2819.2	2836.3
		kVAr	0.0	0.0	1886.5	1860.1
		kVA	3110.9	3043.5	3392.2	3391.8
		pl (%)	71.20	69.66	77.64	77.63

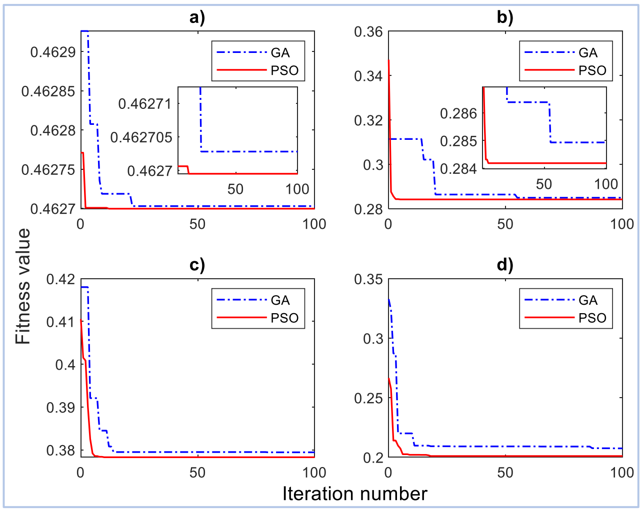

FIGURE 9. Convergence characteristics of the proposed algorithms in case 1C for a) 1 DG placement of Type I; b) 1 DG placement of Type III; c) 2 DGs placement of Type I; d) 2 DGs placement of Type III.

B. PARTICLE SWARM OPTIMIZATION

The PSO algorithm, which was inspired by the social behavior of organisms such as fish breeding and flocks of birds, was first introduced by Kennedy and Eberhart in 1995 [49].

The system (swarm) is initialized with a population of random solutions (particles). Next, generations are updated and optimization is explored using social factors. The particles are randomly oriented toward the best velocities and positions of each particle and its neighbors [50].

General steps of PSO implementation are as follows [51]:

Step 1: n-dimensional initial particles with random positions (χ_i) and velocities (V_i) are created and the iteration counter is set to zero. These terms are formulated as follows.

$$\chi_i = (x_{i1}, \cdots, x_{in}) \tag{29}$$

$$V_i = (v_{i1}, \cdots, v_{in}) \tag{30}$$

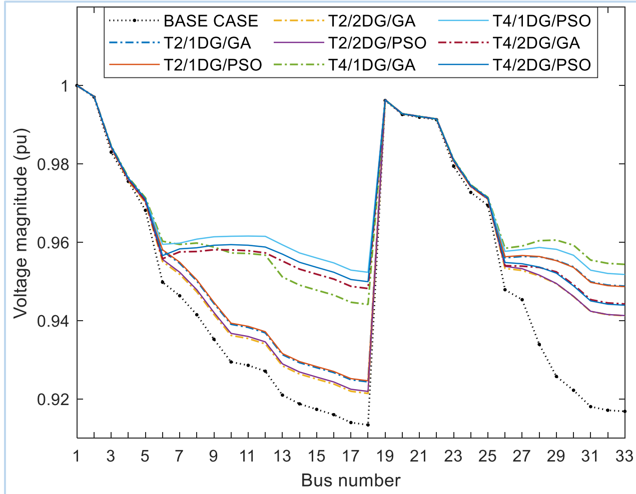

FIGURE 10. Voltage profile comparison for case 1A.

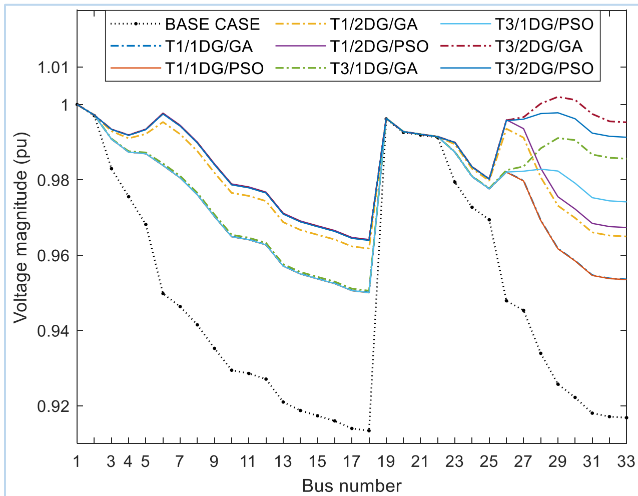

FIGURE 11. Voltage profile comparison for case 1B.

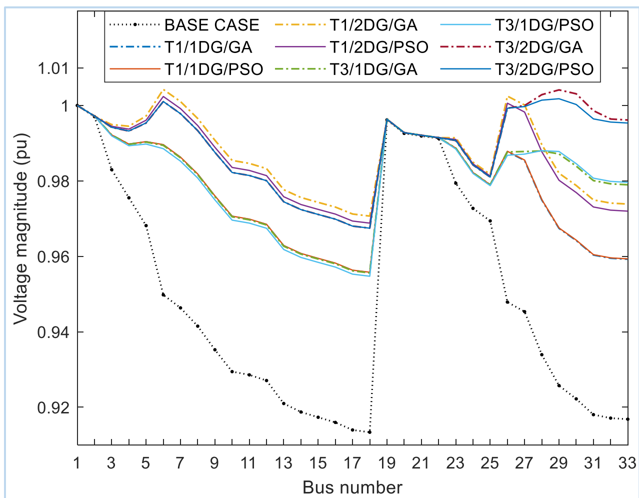

FIGURE 12. Voltage profile comparison for case 1C.

Step 2: Fitness values (F) are calculated for each created particle.

TABLE 6. The effects of optimum solutions on the DS in case study 1.

CASE		DG type	Method	pl (%)	PL (kW)	QL (kVAr)	VDI	Umin (pu)	CPL (%)	CQL (%)	CUmin (%)	Power from the substation kW	kVAr	kVA	%
Base case (No DG)				-	201.99	134.74	0.11642	0.91337	-	-	-	3917.0	2434.7	4612.0	100
1A	1DG	2	GA	23.76	152.38	96.61	0.07397	0.92437	24.56	28.30	1.20	3867.4	1358.4	4099.0	88.9
			PSO	24.48	152.36	96.66	0.07352	0.92464	24.57	28.26	1.23	3867.4	1326.9	4088.7	88.7
		4	GA	17.17	165.32	105.72	0.08360	0.92141	18.15	21.54	0.88	3205.1	2732.8	4211.9	91.3
			PSO	18.65	165.22	105.98	0.08253	0.92192	18.20	21.34	0.94	3146.8	2761.2	4186.5	90.8
	2DG	2	GA	30.30	136.61	83.87	0.04678	0.94412	32.37	37.76	3.37	3851.6	1059.9	3994.8	86.6
			PSO	28.21	134.61	82.45	0.04209	0.95177	33.36	38.81	4.20	3849.6	1149.7	4017.6	87.1
		4	GA	19.17	147.24	90.43	0.05112	0.94425	27.10	32.89	3.38	3108.6	2755.4	4154.0	90.1
			PSO	21.42	146.35	90.31	0.04940	0.94392	27.55	32.98	3.34	3018.9	2798.3	4116.4	89.3
1B	1DG	1	GA	61.46	112.09	77.74	0.03201	0.95008	44.51	42.30	4.02	1141.8	2377.7	2637.7	57.2
			PSO	61.33	112.08	77.72	0.03212	0.95001	44.51	42.32	4.01	1147.3	2377.7	2640.1	57.2
		3	GA	69.11	72.29	53.25	0.01673	0.96176	64.21	60.48	5.30	1250.7	714.8	1440.5	31.2
			PSO	72.68	71.94	53.38	0.01427	0.96415	64.38	60.39	5.56	1151.2	582.2	1290.0	28.0
	2DG	1	GA	62.29	95.76	65.35	0.02180	0.95055	52.59	51.50	4.07	1089.2	2365.4	2604.1	56.5
			PSO	61.39	93.15	62.15	0.02447	0.95004	53.88	53.87	4.01	1126.0	2362.2	2616.8	56.7
		3	GA	72.46	52.61	38.56	0.00962	0.96401	73.95	71.38	5.54	1137.7	575.7	1275.0	27.6
			PSO	72.33	50.98	36.80	0.00986	0.96392	74.76	72.69	5.53	1153.5	558.6	1281.7	27.8
1C	1DG	1	GA	71.36	115.03	80.56	0.02376	0.95570	43.05	40.21	4.63	712.2	2380.6	2484.8	53.9
			PSO	71.52	115.12	80.64	0.02363	0.95579	43.01	40.15	4.64	705.1	2380.6	2482.9	53.8
		3	GA	82.42	74.33	55.94	0.00878	0.97068	63.20	58.49	6.27	764.2	401.9	863.4	18.7
			PSO	79.64	73.14	54.86	0.01017	0.96881	63.79	59.28	6.07	900.0	414.0	990.7	21.5
	2DG	1	GA	71.20	96.08	64.98	0.01777	0.95561	52.43	51.78	4.62	700.2	2365.0	2466.5	53.5
			PSO	69.66	95.27	64.28	0.01846	0.95473	52.84	52.29	4.53	766.8	2364.3	2485.5	53.9
		3	GA	77.64	53.35	39.69	0.00757	0.96747	73.59	70.54	5.92	949.2	453.2	1051.8	22.8
			PSO	77.63	51.65	37.83	0.00756	0.96747	74.43	71.92	5.92	930.4	477.7	1045.8	22.7

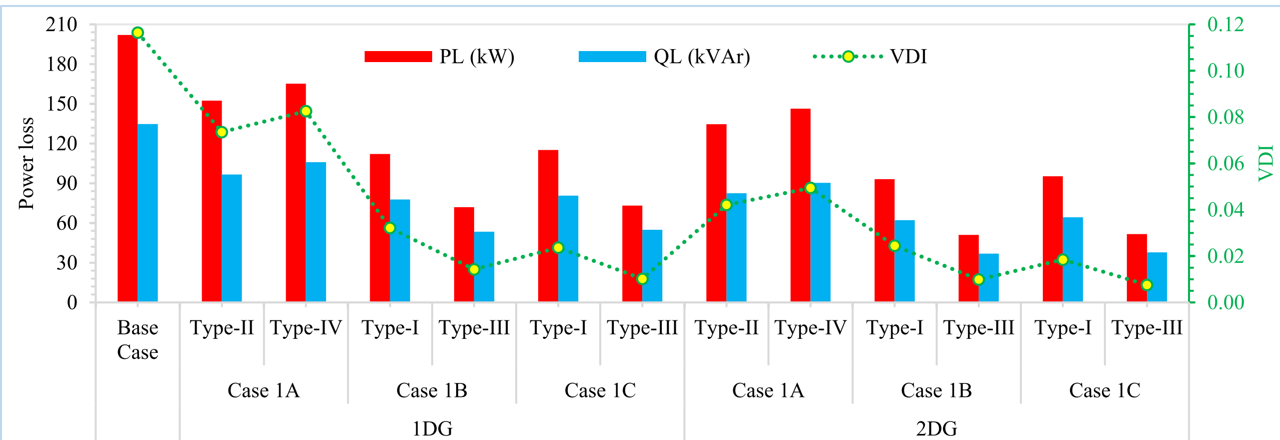

FIGURE 13. Comparison of PSO results such as active power losses, reactive power losses and voltage deviation indexes.

Step 3: $Pbest_i^k$ and $Gbest^k$ are recorded as the local and global best solutions of the problem, respectively [52].

$$Pbest_i^k = \left(Pbest_{i1}^k, \cdots, Pbest_{in}^k\right) \tag{31}$$

$$Gbest^k = \left(Gbest_1^k, \cdots, Gbest_n^k\right) \tag{32}$$

Step 4: The particle velocity and position are updated using Eqs. (33) and (34) [53]. The velocity and position updates for each particle are shown in Fig. 2 [54], [55].

$$V_i^{k+1} = \omega V_i^k + c_1 r_1 \left(Pbest_i^k - x_i^k\right) + c_2 r_2 \left(Gbest^k - x_i^k\right) \tag{33}$$

$$x_i^{k+1} = x_i^k + V_i^{k+1} \tag{34}$$

where, n is the number of particles; k is the iteration k^{th}; V_i^k is the velocity of particle i at iteration k; r_1 and r_2 are random numbers between 0 and 1; c_1 and c_2 are acceleration factors. ω is the weight coefficient and calculated as follows [52].

$$\omega = \omega_{max} - \frac{\omega_{max} - \omega_{min}}{k_{max}} k \tag{35}$$

where, ω_{min} is the minimum (final) weight; ω_{max} is the maximum (initial) weight; k_{max} is the maximum number of iterations.

Step 5: The fitness values of all updated particles are calculated and these processes are repeated until the stopping criteria are satisfied.

Step 6: When the stopping criteria are satisfied, the algorithm is terminated and the optimum results are printed.

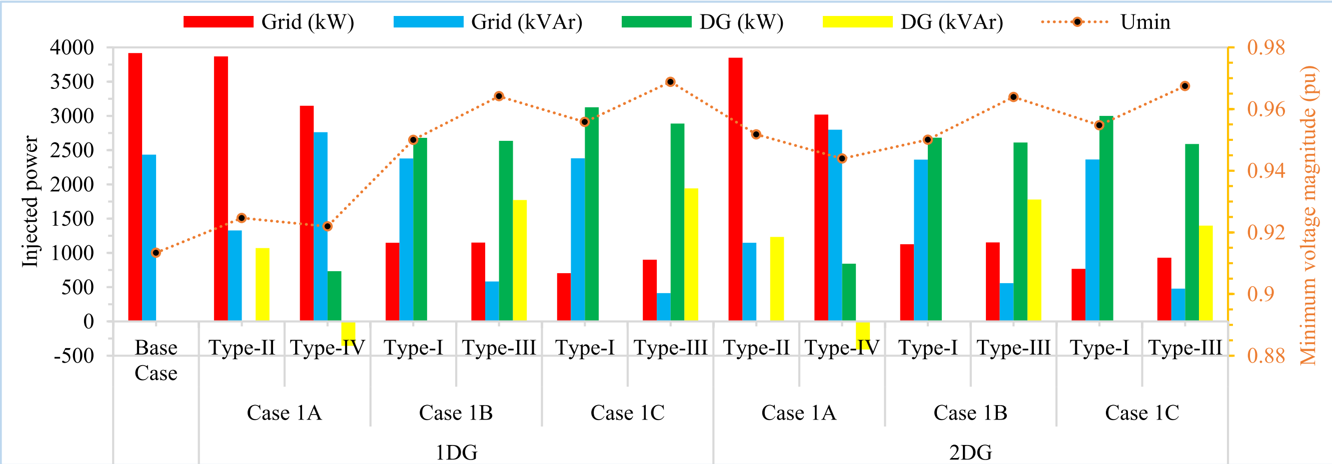

FIGURE 14. Comparison of PSO results such as injected active and reactive powers from SS and DGs, and minimum voltage magnitude values.

TABLE 7. Comparison of the proposed methods and other methods in the literature studies for 1 DG placement.

Year	Method	LDG (@bus)	SDG (kVA)	PDG (kW)	QDG (kVAr)	PF	PL (kW)	QL (kVAr)	Umin (pu)
2010	GA [8]	6	2380	2380	0	1	132.64	NA	0.92
2013	DAPSO [2]	8	1212	1212	0	1	127.17	NA	0.9349
2014	HPSO [20]	14	1747.7	1485.5	920.7	0.85	112.8	81.92	NA
2015	SA [15]	31	168	168	0	1	180.37	NA	NA
2015	AM [19]	24	1656.1	1585.2	479.6	0.9572	130.86	NA	NA
2016	BA [16]	15	816.3	816.3	0	1	137.2	NA	NA
2018	ALOA [59[	30	1940.3	1746.3	845.8	0.9	78.43	58.97	0.9386
2018	ALOA [36]	6	2590.2	2590.2	0	1	111.03	NA	0.9424
2019	PPSO [1]	6	2574.3	2574.3	0	1	103.90	NA	NA
2019	CSFS [17]	6	2590	2590	0	1	111.02	NA	NA
2020	PPA [14]	6	3640	3640	0	1	91.09	NA	0.96
2021	BPSO-WOA [60]	18	2054.4	1645.5	1230	0.8010	94.01	63.45	NA
2021	EGOA [33]	17	902.9	902.9	0	1	141.12	NA	0.9302
2021	PSO [52]	3	592.1	592.1	0	1	130.03	NA	NA
2022	**Proposed GA**	**6**	**3019.8**	**2536.6**	**1638.5**	**0.84**	**72.29**	**53.25**	**0.9618**
2022	**Proposed PSO**	**6**	**3175.6**	**2535.7**	**1771.2**	**0.83**	**71.94**	**53.38**	**0.9642**

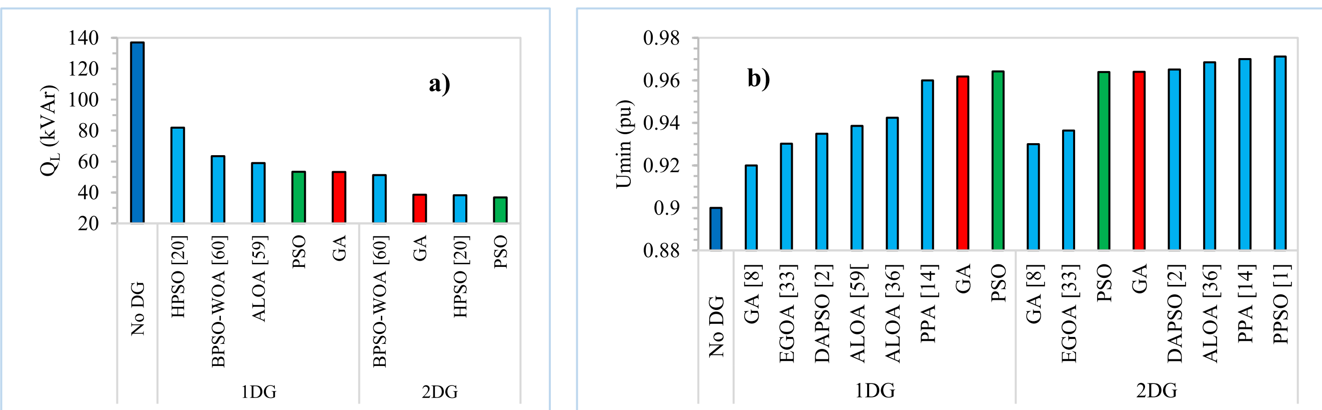

FIGURE 15. Comparisons with the studies in the literature for a) reactive power losses and; b) minimum voltage magnitude values.

TABLE 8. Comparison of the proposed methods and other methods in the literature studies for 2 DGs placement.

Year	Method	L-DG1 (@bus)	P-DG1 (kW)	Q-DG1 (kVAr)	L-DG2 (@bus)	P-DG (kW)	Q-DG2 (kVAr)	Total S-DG (kVA)	PL (kW)	QL (kVAr)	Umin (pu)
2010	GA [8]	6	1718	0	8	840	0	2558	96.58	NA	0.93
2013	DAPSO [2]	13	1227	0	32	738	0	1965	95.93	NA	0.9651
2014	HPSO [20]	17	742.8	460.3	31	742.8	460.3	1747.7	52.72	38.15	NA
2015	SA [15]	30	79.5	0	13	96	0	175.5	178.28	NA	NA
2015	AM [19]	6	1120.3	1053.8	14	775	370.3	2370.6	131.53	NA	NA
2016	BA [16]	15	952.4	0	25	952.4	0	1904.7	112.88	NA	NA
2018	ALOA [36]	13	851.5	0	30	1157.6	0	2009.1	87.17	NA	0.9685
2019	PPSO [1]	13	846.1	0	30	1158.2	0	2004.3	85.80	NA	0.9712
2019	CSFS [17]	13	852	0	30	1158	0	2010	87.17	NA	NA
2020	PPA [14]	3	1271	0	6	2255	0	3526	64.11	NA	0.97
2021	BPSO-WOA [60]	18	1779.9	900	33	279.1	600	2547.4	86.55	51.23	NA
2021	EGOA [33]	17	962.3	0	18	184.5	0	1146.8	128.56	NA	0.9364
2021	PSO [52]	18	438.6	0	33	394.7	0	833.2	86.12	NA	NA
2022	**Proposed GA**	**32**	**469.7**	**460.5**	**6**	**2160.2**	**1302.4**	**3166.1**	**52,61**	**38,56**	**0,964**
2022	**Proposed PSO**	**30**	**245.2**	**500.5**	**6**	**2367.2**	**1277.7**	**3160.2**	**50,98**	**36,8**	**0,9639**

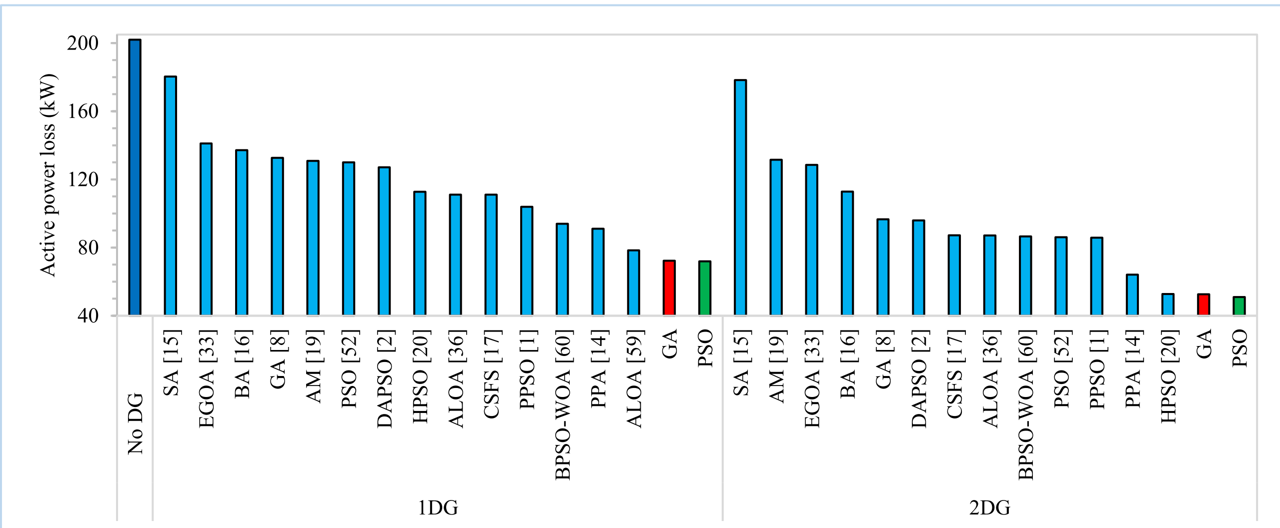

FIGURE 16. Active power loss comparison of the proposed methods and the other methods in the literature.

A simplified flowchart [56] and the parameters of the PSO used in this study are shown in Fig. 3 and in Table 2.

IV. CASE STUDIES AND RESULTS

In this study, a well-known IEEE 33-bus radial power distribution system is selected as the test system. A single-line diagram of the DS with 32 branches is shown in Fig. 4 [57], and the data consisting of resistance, reactance and maximum current-carrying capacity values of these 32 branches and connected loads to the power system are given in Appendix Table 14 [58]. The rated voltage is 12.66 kV and the total active and reactive loads are 3715 kW and 2300 kVAr at peak time, respectively [20].

Two heuristic methods, GA and PSO, are used for the optimal placement of single and double DGs in all case studies except for the base case study.

A. BASE CASE STUDY

In this case, the IEEE 33-bus RDN before DG integration was examined for comparison with other cases after DG integration. According to the power flow results at peak time, the voltage magnitudes of the buses are shown in Fig. 5, and the total active and reactive losses of the power system are 201.99 kW and 134.77 kVAr, respectively. The worst or minimum voltage is 0.91337 pu at the 18th bus, and VDI is 0.11642 in the base case.

The seasonal load curve is shown in Appendix Table 15 and graphically in Fig. 6 [34]. While annual active and reactive energy losses were calculated as 680.8 MWh and 453.8 MVArh, the energy of 20.5 GWh active and 12.7 GVArh reactive were injected from the substation (SS) in a year. The worst voltage corresponds to the value at the peak load time, and the total VDI is calculated 4.29 per year.

TABLE 9. Convergence comparison of the proposed methods and the other methods in the literature.

Test system	Reference	Method	DG number	DG Type	Convergence	Max. iter
IEEE 33-bus RDN	Fig. 10 in [1]	PSO PPSO	3 DG	Type I	195 45	200
	Fig. 3 in [17]	CSFS	-	Type I	100	100
	Fig. 16 in [4]	PSO HHO HHO-PSO	2 PV	Type I	100 85 18	100
		PSO HHO HHO-PSO	3 WT	Type III	97 18 47	
	Fig. 7 in [14]	PPA	1DG 2DG 3DG 4DG	Type I	16 17 18 21	30
	Fig. 12 in [20]	HPSO	1DG	Type III	70	-
	Fig.4 and Fig. 6 in [36]	ALOA	1DG 2DG	Type I	15 18	100
	Fig. 12 in [21]	CO	2DG	Type III	425	500
	This paper	**GA**	1DG 2DG	Min. 10, avg. 30 and max. 55 Min. 43, avg. 67 and max. 90		100
		PSO	1DG 2DG	Min. 2, avg. 5 and max. 7 Min.6, avg.11 and max. 18		
Portuguese 94-bus RDN	Fig. 8 in [12]	PPSO-GSA	1PV 2PV 3PV	Type I	10 45 65	200
13-bus RDN	Fig.1 and Fig. 2 in [11]	GSA	1DG 2DG	Type I	60 140	300
		PSO	1DG 2DG		120 200	

TABLE 10. Optimal CS placement solutions.

DG number and type		Method	Conventional DG		
			pf	Location	kVAp
1DG	upf	GA	1	6	2576
		PSO	1	6	2629
	opf	GA	0.865	6	3170
		PSO	0.83	6	3168
2DG	upf	GA	1	29	383
			1	6	2436
		PSO	1	29	102
			1	6	2547
	opf	GA	0.7259	32	711
			0.8603	6	2467
		PSO	0.33	30	580
			0.89	6	2876

TABLE 11. Optimal PV placement solutions.

DG number and type		Method	PV DG		
			pf	Location	kVAp
1DG	upf	GA	1	6	2322
		PSO	1	6	2379
	opf	GA	0.840	6	2582
		PSO	0.83	6	2908
2DG	upf	GA	1	29	424
			1	6	1915
		PSO	1	29	42
			1	6	2337
	opf	GA	0.6059	30	376
			0.84	6	2486
		PSO	0.63	30	453
			0.85	6	2423

TABLE 12. Optimal WT placement solutions.

DG number and type		Method	WT DG		
			pf	Location	kVAp
1DG	upf	GA	1	6	1718
		PSO	1	6	1802
	opf	GA	0.845	6	1873
		PSO	0.83	6	1906
2DG	upf	GA	1	29	195
			1	6	1584
		PSO	1	29	71
			1	6	1741
	opf	GA	0.6092	30	456
			0.8267	6	1781
		PSO	0.37	30	400
			0.9	6	1851

B. CASE STUDY 1: FOR PEAK LOAD

This case study is for the peak load and has three subcases to optimize the allocation of all DGs in four types under different objective functions and constraints. The subcases are as follows.

Case 1A: Minimization of active power loss with voltage constraint-1 using DG types II and IV.

Case 1B: Minimization of active power loss with voltage constraint-2 using DG types I and III.

Case 1C: Multi-objective problem (minimizing active and reactive power losses, and maximizing voltage profile improvement) with voltage constraint-2 using DG types I and III.

The convergence graphs of the proposed algorithms for Case 1A, 1B and 1C are shown in Fig. 7, Fig. 8 and Fig. 9, respectively. The optimum solutions for DG allocation by the GA and PSO are listed in Tables 3, 4 and 5 for the subcases.

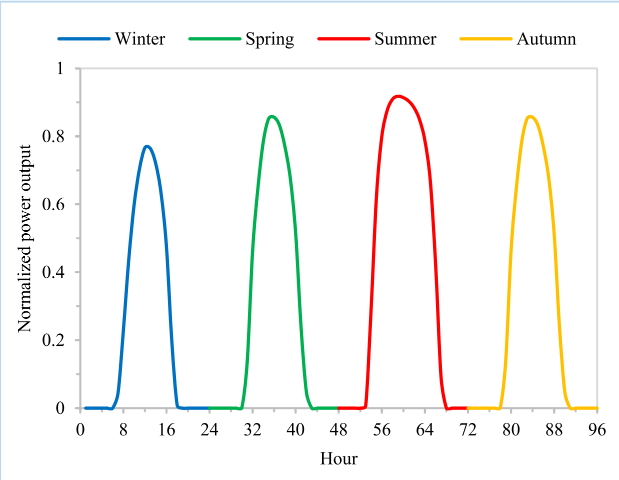

FIGURE 17. Seasonal output of PV.

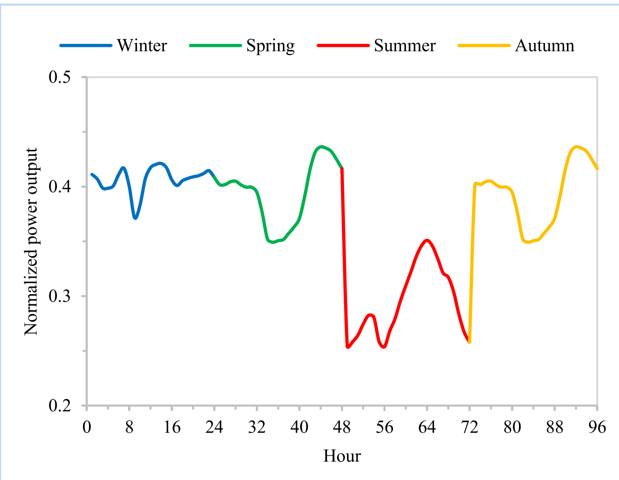

FIGURE 18. Seasonal output of WT.

The values with a negative sign of DG reactive power in Table 3 indicate that the DG consumes reactive power.

After DG placement, the effects of DG allocation are observed by calculating various parameters such as active losses, reactive losses, minimum busbar voltages, voltage deviation indexes of the power DS, and powers drawn from the main SS. Comparisons of the effects of all subcases using the proposed methods with each other and with base case are presented in Table 6. The effects of DG placement on voltage profile are shown in Fig. 10, Fig. 11 and Fig. 12 for Cases 1A, 1B and 1C, respectively.

Table 6 shows that PSO offers better solutions than GA for all subcases. Accordingly, the comparison of the solutions produced by PSO for the subcases with each other and with the base case is shown in Fig. 13 and Fig. 14.

Fig. 13 shows a comparison of the active power losses, reactive power losses and voltage deviation indexes, and Fig. 14 shows a comparison of the active and reactive power injection of DGs and SS, and minimum voltage magnitude value of the test system.

Comparisons of the proposed methods with the other methods in the literature in various aspects such as DG

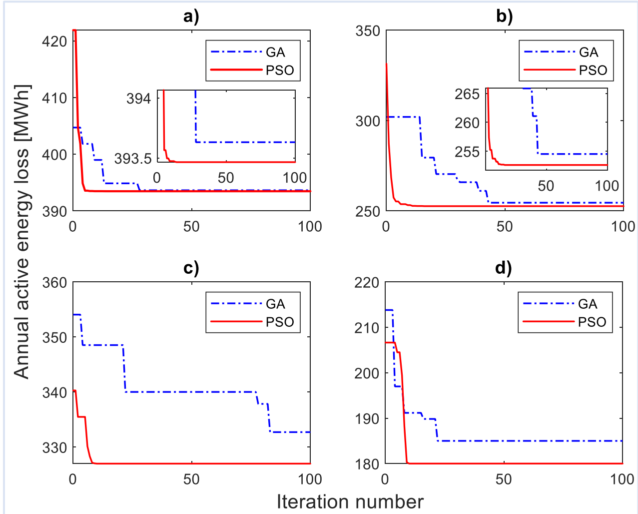

FIGURE 19. Convergence characteristics of the proposed algorithms in case 2 for a) 1 CS placement of Type I; b) 1 CS placement of Type III; c) 2 CSs placement of Type I; d) 2 CSs placement of Type III.

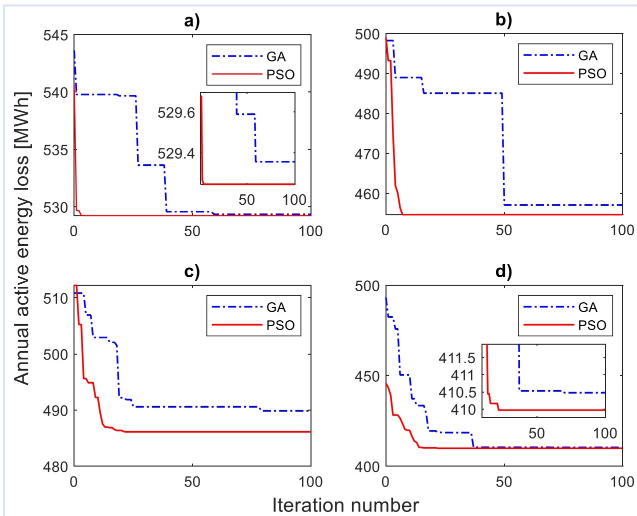

FIGURE 20. Convergence characteristics of the proposed algorithms in case 2 for a) 1 PV placement of Type I; b) 1 PV placement of Type III; c) 2 PVs placement of Type III; d) 2 PVs placement of Type III.

size, location and pf, active and reactive losses, and minimum voltage value are given in Tables 7 and 8 for 1 DG and 2 DGs placements, respectively. In addition, a comparison of the proposed methods and the other methods in the literature in terms of reactive power losses, minimum bus voltages, and active power losses are shown graphically in Fig. 15 and Fig. 16, respectively.

Also, comparison of the convergence and maximum iteration numbers with those in literature is listed in Table 9.

C. CASE STUDY 2: FOR SEASONAL LOADS

In this case, optimum DG allocation was made to minimize the annual active energy loss considering the seasonal variation of loads and power outputs of the DGs. Conventional sources (CSs) and RESs such as PV and WT were used as DGs. The normalized seasonal power outputs of PV and WT

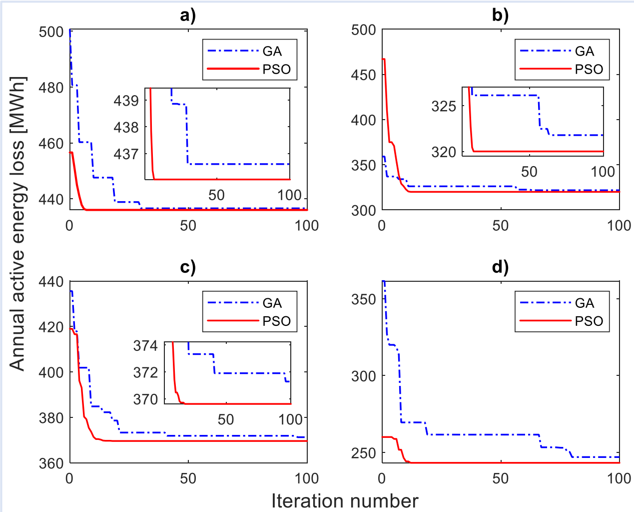

FIGURE 21. Convergence characteristics of the proposed algorithms in case 2 for a) 1 WT placement of Type I; b) 1 WT placement of Type III; c) 2 WTs placement of Type I; d) 2 WTs placement of Type III.

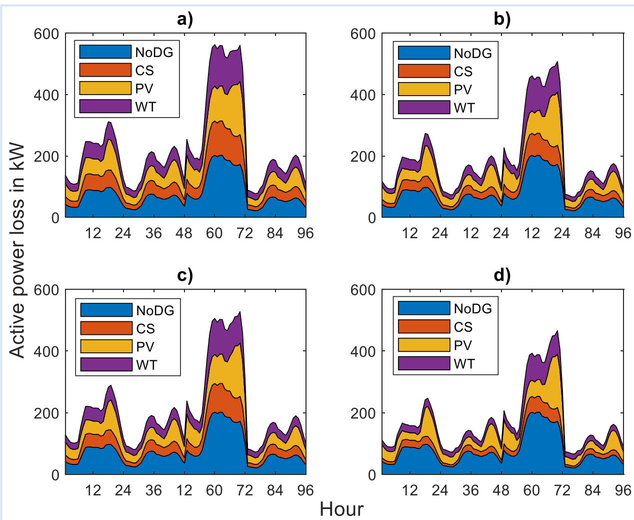

FIGURE 22. Comparison of active power loss minimization by PSO in case 2 for a) 1 DG placement of Type I; b) 1 DG placement of Type III; c) 2 DGs placement of Type I; d) 2 DGs placement of Type III.

are given in Appendix Tables 16 and 17, and graphically in Fig. 17 and Fig. 18, respectively.

To reduce carbon emissions, fuel-based CSs were prevented by supplying energy to the SS. On the other hand, RESs can be supplied to the SS to avoid wasting their excess energy.

All DGs were operated at upf as type I and opf as type III. The optimal solutions of DG allocation by GA and PSO to minimize annual active energy losses are listed in Tables 10, 11 and 12 for CS, PV and WT, respectively. The convergence characteristics of the proposed methods are shown in Fig. 19, Fig. 20 and Fig. 21.

Table 13 presents a comparison for the effects of optimum solutions for CS, PV and WT allocation on the DS. The best solutions were also obtained with PSO and the results are compared in Fig. 22-25 for active and reactive power losses,

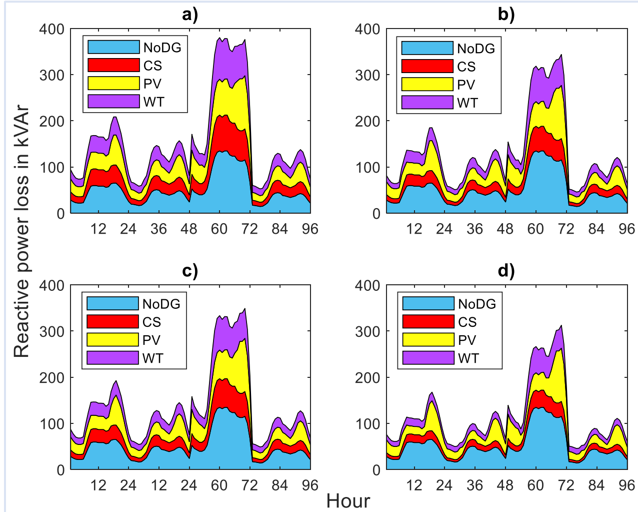

FIGURE 23. Comparison of reactive power loss minimization by PSO in case 2 for a) 1 DG placement of Type I; b) 1 DG placement of Type III; c) 2 DGs placement of Type I; d) 2 DGs placement of Type III.

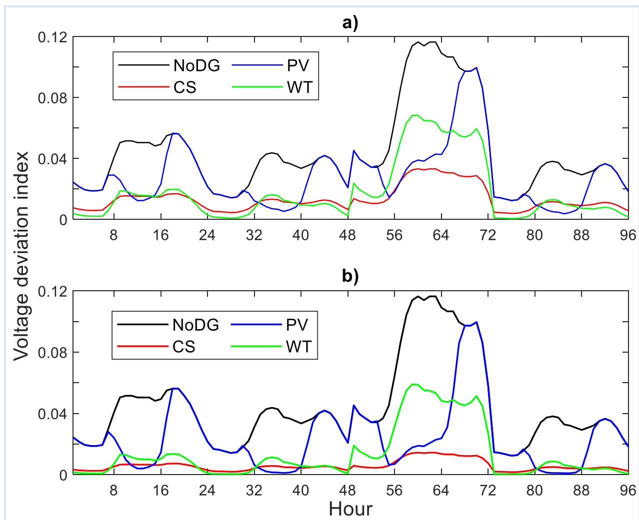

FIGURE 24. Comparison of VDI obtained by PSO in case 2 for 1 DG placement of a) Type I; b) Type III.

and VDI after 1DG and after 2DG, respectively. Power injection of SS and DG, and peak demand of the system before and after DG integration is shown in Fig. 26. A comparison of the annual active energy losses obtained by GA and PSO is shown in Fig. 27

V. DISCUSSION

In case study 1, Type IV DGs, it was able to provide optimum solution at lowest pl among all types and was between 17% and 21%. This was followed by Type II with 23-30%, Type I with 61-71%, and Type III with the highest pl of 69-82%.

Owing to the proper constraints of this study, optimum solutions could be provided for all DG types and no negative effects were observed. The size of the positive effects on the grid varied depending on the characteristics of the DG type. The best results for case study 1 were obtained with 2 DGs of

TABLE 13. The effects of optimum DG placements on the DS in case study 2.

DG number	pf	Method	Energy losses		VDI	U (pu)		Energy from DG			Energy from SS		
			MWh	MVArh		min	max	MWh	MVArh	pl (%)	MWh	MVArh	pl (%)
No DG	-	-	680.82	453.84	4.29224	0.91337	1	-	-	-	20460	12699	100
1CS	upf	GA	393.63	272.19	1.32476	0.94866	1	13714	0	56.95	6459	12517	58.49
		PSO	393.46	272.48	1.28098	0.94935	1	13999	0	58.13	6173	12518	57.96
	opf	GA	254.51	188.78	0.55432	0.96399	1	14599	8468	70.09	5435	3966	27.94
		PSO	252.61	187.35	0.55384	0.96404	1	13999	9407	70.04	6033	3025	28.03
2CS	upf	GA	332.72	223.78	0.89294	0.95182	1	15012	0	62.34	5100	12469	55.94
		PSO	327.00	217.93	0.96771	0.94961	1	14103	0	58.57	6003	12463	57.45
	opf	GA	185.01	135.87	0.37263	0.96398	1.00109	14048	9299	69.96	5916	3083	27.70
		PSO	180.01	131.08	0.31635	0.96636	1.00046	14645	9896	73.40	5314	2480	24.35
1PV	upf	GA	529.36	356.27	2.71576	0.91989	1	6730	0	27.95	13581	12602	76.94
		PSO	529.25	356.44	2.68854	0.91989	1	6895	0	28.63	13420	12602	76.45
	opf	GA	457.16	311.66	2.41026	0.91989	1.00793	6287	4061	31.08	13949	8496	67.82
		PSO	454.74	311.62	2.28945	0.91989	1.01245	6997	4702	35.01	13253	7924	64.12
2PV	upf	GA	489.88	323.96	2.49880	0.91989	1	6779	0	28.15	13494	12569	76.58
		PSO	486.14	320.96	2.44789	0.91989	1	6898	0	28.64	13376	12566	76.22
	opf	GA	410.48	276.80	2.10518	0.91989	1.01150	6712	4776	34.21	13477	7839	64.74
		PSO	409.97	276.36	2.10364	0.91989	1.01170	6798	4720	34.37	13396	7880	64.54
1WT	upf	GA	436.60	297.16	1.78226	0.93112	1.00315	12843	0	53.33	7576	12542	60.85
		PSO	436.03	297.57	1.69452	0.93189	1.00417	13473	0	55.95	7064	12543	59.78
	opf	GA	321.78	225.87	1.31495	0.93578	1.00921	11833	7489	58.15	8344	5046	40.49
		PSO	320.00	224.99	1.28411	0.93613	1.00968	11829	7949	59.19	8345	4649	39.67
2WT	upf	GA	371.28	244.14	1.39147	0.93168	1.00389	13300	0	55.23	7145	12489	59.75
		PSO	369.61	243.01	1.33978	0.93198	1.00429	13546	0	56.25	6952	12488	59.35
	opf	GA	247.04	170.81	0.77651	0.93931	1.01402	13084	10194	68.88	7194	2984	32.34
		PSO	243.29	168.09	0.79413	0.93880	1.01335	13564	8813	67.17	6820	3927	32.68

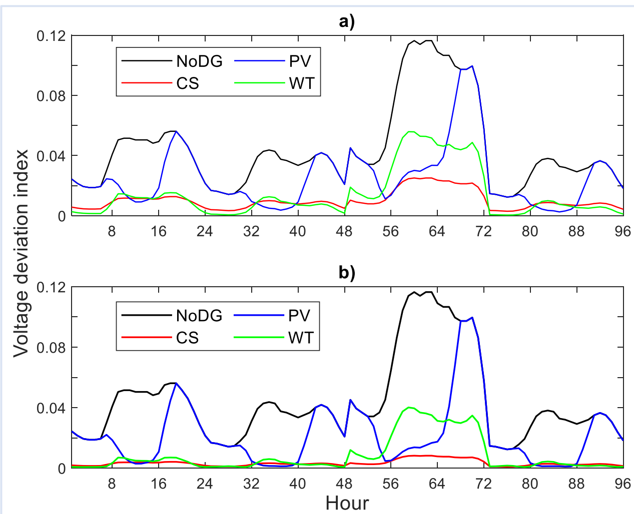

FIGURE 25. Comparison of VDI obtained by PSO in case 2 for 2 DGs placement of a) Type I; b) Type III.

Type III in case 1B and the active losses were reduced from 201.99 kW to 50.98 kW with a %74.76 reduction by PSO and to 52.61 kW with a %73.95 by GA. In addition, VDI was reduced from 0.11642 to 0.00962 and 0.00986, and the minimum voltage value was improved from 0.91337 pu to 0.96401 pu and 0.96392 pu ($>0.95pu$) by the GA and PSO, respectively. It can be seen from Table 7-9 and Fig. 15-16 that the solutions of our proposed algorithms outperform those in the literature in terms of active and reactive power loss minimization, voltage profile enhancement and fast convergence.

In case study 2, annual active energy loss was reduced from 453.84 MWh to 327 MWh, 486.14 MWh and 369.31 MWh by operating the CS, PV and WT at upf, while it was reduced to 180.01 MWh, 409.97 MWh and 243.29 MWh by operating the DGs at opf, respectively. VDI was reduced from 4.29 to

TABLE 14. Data of IEEE 33-bus RDN [58].

Line	From (bus)	To (bus)	R (Ω)	X (Ω)	Pd (kW)	Qd (kVAr)	Imax (A)
1	1	2	0.0922	0.0470	100	60	400
2	2	3	0.4930	0.2511	90	40	400
3	3	4	0.3660	0.1864	120	80	400
4	4	5	0.3811	0.1941	60	30	400
4	5	6	0.8190	0.7070	60	20	400
6	6	7	0.1872	0.6188	200	100	300
7	7	8	0.7114	0.2351	200	100	300
8	8	9	1.0300	0.7400	60	20	200
9	9	10	1.0440	0.7400	60	20	200
10	10	11	0.1966	0.0650	45	30	200
11	11	12	0.3744	0.1238	60	35	200
12	12	13	1.4680	1.1550	60	35	200
13	13	14	0.5416	0.7129	120	80	200
14	14	15	0.5910	0.5260	60	10	200
15	15	16	0.7463	0.5450	60	20	200
16	16	17	1.2890	1.7210	60	20	200
17	17	18	0.7320	0.5740	90	40	200
18	2	19	0.2640	0.2565	90	40	200
19	19	20	1.5042	1.3554	90	40	200
20	20	21	0.4095	0.4784	90	40	200
21	21	22	0.7089	0.9373	90	40	200
22	3	23	0.4512	0.3083	90	50	200
23	23	24	0.8980	0.7091	420	200	200
24	24	25	0.8960	0.7011	420	200	200
25	6	26	0.2030	0.1034	60	25	300
26	26	27	0.2842	0.1447	60	25	300
27	27	28	1.0590	0.9337	60	20	300
28	28	29	0.8042	0.7006	120	70	200
29	29	30	0.5075	0.2585	200	600	200
30	30	31	0.9744	0.9630	150	70	200
31	31	32	0.3105	0.3619	210	100	200
32	32	33	0.3410	0.5302	60	40	200

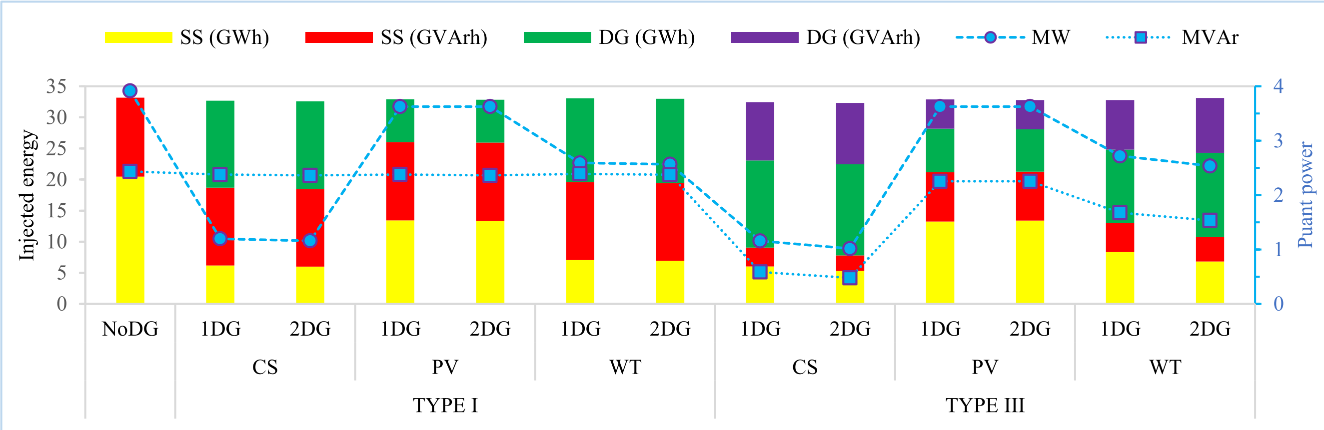

FIGURE 26. Power injections of SS and DGs, and peak demands of the system after and before DGs.

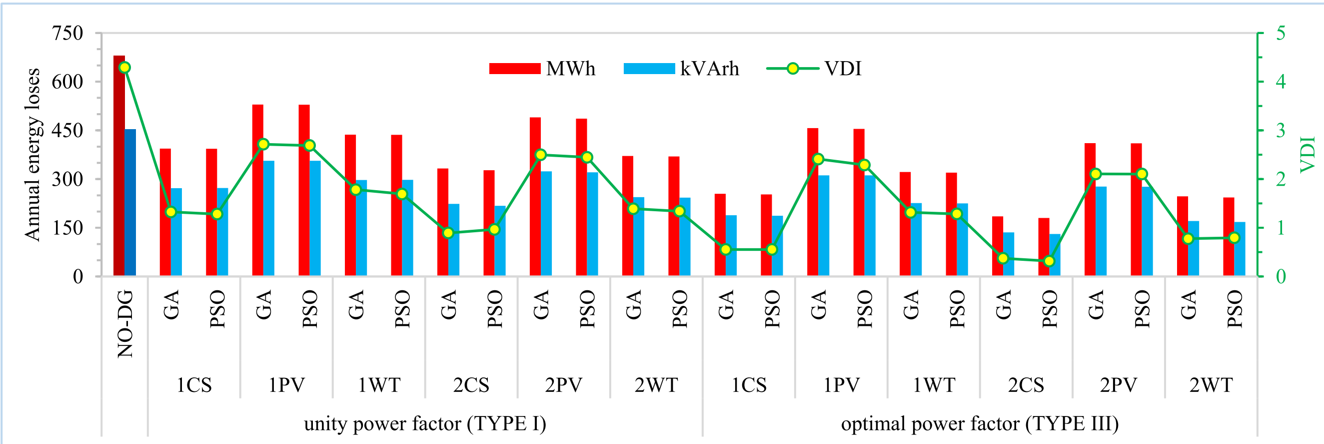

FIGURE 27. Comparison for annual active and reactive energy losses, and VDI.

0.97, 2.45 and 1.34 by operating the DGs at upf and to 0.32, 2.10 and 0.79 at opf for CS, PV and WT, respectively. The minimum voltage improved from 0.91337 pu to 0.96636 pu for CS, 0.91989 pu for PV and 0.93880 pu for WT.

Although the GA and PSO ensured very close results in all cases, the best results were obtained with PSO. The convergence graphs clearly show that PSO converges faster than GA.

VI. CONCLUSION

This study proposes two heuristic optimization algorithms for determining the optimum sizes, locations and operating power factors of DGs to minimize power losses and voltage deviation. The validity of the suggested methods was tested on the IEEE 33-bus radial test system with various types of DGs, objective functions and constraints.

The following are the main conclusions based on the analyses performed in this study.

- Type IV DGs provide the lowest optimum solution due to its reactive power consumption.
- Type III DGs offer the best results because of their ability to provide both active and reactive powers.
- The annual active energy loss reductions of operating DGs at opf were 73.6%, 39.8 % and 64.3% for CS, PV and WT, respectively. For operating DGs at upf, the reductions are less than 30% compared to operating at opf.
- The best seasonal results were obtained with power-output-controllable CSs, and the worst results were obtained with PVs because of uneven irradiation distribution.
- Because WTs provide near-optimal results owing to the relatively regular distribution of wind speed and reduce emissions due to being renewable energy-based, they are the most appropriate DG placement solution.
- Operating DGs at opf in accordance with the IEEE 1547 standard yielded better results than those operating at upf.
- The proposed methods have proven their robustness and applicability by providing better results than studies in the literature in terms of reducing power losses, improving the voltage profile and fast convergence, particularly PSO.

The results show that location, size, and the operating power factor of DG are very important in DG placement, and

TABLE 15. Seasonal loads.

Hour	Winter	Spring	Summer	Autumn
12-1am	0.4757	0.3969	0.64	0.3717
1-2	0.4473	0.3906	0.6	0.3658
2-3	0.426	0.378	0.58	0.354
3-4	0.4189	0.3654	0.56	0.3422
4-5	0.4189	0.3717	0.56	0.3481
5-6	0.426	0.4095	0.58	0.3835
6-7	0.5254	0.4536	0.64	0.4248
7-8	0.6106	0.5355	0.76	0.5015
8-9	0.6745	0.5985	0.87	0.5605
9-10	0.6816	0.6237	0.95	0.5841
10-11	0.6816	0.63	0.99	0.59
11-12pm	0.6745	0.6237	1	0.5841
12-1	0.6745	0.5859	0.99	0.5487
1-2	0.6745	0.5796	1	0.5428
2-3	0.6603	0.567	1	0.531
3-4	0.6674	0.5544	0.97	0.5192
4-5	0.7029	0.567	0.96	0.531
5-6	0.71	0.5796	0.96	0.5428
6-7	0.71	0.6048	0.93	0.5664
7-8	0.6816	0.6174	0.92	0.5782
8-9	0.6461	0.6048	0.92	0.5664
9-10	0.5893	0.567	0.93	0.531
10-11	0.5183	0.504	0.87	0.472
11-12am	0.4473	0.441	0.72	0.413

TABLE 16. Seasonal PV outputs.

Hour	Winter	Spring	Summer	Autumn
1	0	0	0	0
2	0	0	0	0
3	0	0	0	0
4	0	0	0	0
5	0	0	0	0
6	0	0.001535274	0.287908553	0.001535274
7	0.043500164	0.136744096	0.621574290	0.136744096
8	0.229020093	0.462591393	0.799845285	0.462591393
9	0.437429308	0.649662512	0.876330783	0.649662512
10	0.599329978	0.785687141	0.909453696	0.785687141
11	0.704848050	0.852694211	0.917958954	0.852694211
12	0.766418623	0.856292732	0.913951673	0.856292732
13	0.764404534	0.832127579	0.903577597	0.832127579
14	0.720392139	0.769940423	0.883978865	0.769940423
15	0.632092429	0.676451831	0.849403341	0.676451831
16	0.474469935	0.514273888	0.787477127	0.514273888
17	0.195542111	0.238276554	0.669292662	0.238276554
18	0.007911205	0.046628199	0.419883670	0.046628199
19	0	0	0	0
20	0	0	0	0
21	0	0	0	0
22	0	0	0	0
23	0	0	0	0
24	0	0	0	0

when properly allocated, it significantly reduces losses and carbon emissions, and improves the voltage profile, reliability and resilience of the system.

In future work, the following applications for optimal DG allocation problems can be considered:

- Apply the proposed algorithms to one or more larger test systems such as IEEE 69, 118-bus or practical RDNs.
- Allocate DGs with energy storage systems or electric vehicles, especially for PV installation.

TABLE 17. Seasonal WT outputs.

Hour	Winter	Spring	Summer	Autumn
1	0.411124532	0.401851742	0.254110433	0.401851742
2	0.406881657	0.401799127	0.258233553	0.401799127
3	0.398686927	0.404358915	0.264226866	0.404358915
4	0.398534253	0.404974345	0.274451570	0.404974345
5	0.400680850	0.401619126	0.282398354	0.401619126
6	0.410832705	0.399443601	0.280672381	0.399443601
7	0.416859558	0.399436198	0.258194797	0.399436198
8	0.400153100	0.394812914	0.253686364	0.394812914
9	0.371637762	0.376250384	0.268231479	0.376250384
10	0.382497545	0.352071689	0.279553287	0.352071689
11	0.406806581	0.349255802	0.295657644	0.349255802
12	0.417240711	0.350561839	0.309444262	0.350561839
13	0.420263348	0.351750483	0.322607201	0.351750483
14	0.421119576	0.357423014	0.336486843	0.357423014
15	0.417262384	0.363169032	0.346259267	0.363169032
16	0.406186703	0.370917080	0.350974352	0.370917080
17	0.401032268	0.391260124	0.345847828	0.391260124
18	0.405383810	0.415633638	0.334412592	0.415633638
19	0.407464043	0.431804041	0.321313159	0.431804041
20	0.408925092	0.436268361	0.317164403	0.436268361
21	0.409920451	0.435156506	0.304029385	0.435156506
22	0.412017311	0.432073180	0.283189840	0.432073180
23	0.414529297	0.424703352	0.266978732	0.424703352
24	0.408389606	0.416414107	0.257877269	0.416414107

- Examine the effects on power quality, reliability and protection indices.
- Perform economic and environmental analyzes.
- Study using load and generation data including all hours of the year.
- Use recently developed heuristic optimization algorithms or hybrid applications of the existing algorithms.

APPENDIX

See Tables 14–17.

ACKNOWLEDGMENT

The authors declare that they have no conflicts of interest.

REFERENCES

[1] Z. Ullah, S. Wang, and J. Radosavljević, "A novel method based on PPSO for optimal placement and sizing of distributed generation," *IEEJ Trans. Electr. Electron. Eng.*, vol. 14, no. 12, pp. 1754–1763, Dec. 2019, doi: 10.1002/tee.23001.

[2] H. Manafi, N. Ghadimi, M. Ojaroudi, and P. Farhadi, "Optimal placement of distributed generations in radial distribution systems using various PSO and DE algorithms," *Electron. Elect. Eng.*, vol. 19, no. 10, pp. 53–57, 2013, doi: 10.5755/j01.eee.19.10.1941.

[3] T. Ackermann, G. Andersson, and L. Söder, "Distributed generation: A definition," *Electr. Power Syst. Res.*, vol. 57, no. 3, pp. 195–204, Apr. 2001, doi: 10.1016/S0378-7796(01)00101-8.

[4] M. R. Elkadeem, M. Abd Elaziz, Z. Ullah, S. Wang, and S. W. Sharshir, "Optimal planning of renewable energy-integrated distribution system considering uncertainties," *IEEE Access*, vol. 7, pp. 164887–164907, 2019, doi: 10.1109/ACCESS.2019.2947308.

[5] D. Q. Hung, N. Mithulananthan, and R. C. Bansal, "Analytical expressions for DG allocation in primary distribution networks," *IEEE Trans. Energy Convers.*, vol. 25, no. 3, pp. 814–820, Sep. 2010, doi: 10.1109/TEC.2010.2044414.

[6] IEEE Standard Association, *Standard for Interconnection and Interoperability of Distributed Energy Resources With Associated Electric Power Systems Interfaces*, IEEE Standard 1547-2018, 2018, doi: 10.1109/IEEESTD.2018.8332112.

[7] M. F. Akorede, H. Hizam, and E. Pouresmaeil, "Distributed energy resources and benefits to the environment," *Renew. Sustain. Energy Rev.*, vol. 14, pp. 724–734, Feb. 2010, doi: 10.1016/j.rser.2009.10.025.
[8] T. N. Shukla, S. P. Singh, V. Srinivasarao, and K. B. Naik, "Optimal sizing of distributed generation placed on radial distribution systems," *Electr. Power Compon. Syst.*, vol. 38, no. 3, pp. 260–274, 2010, doi: 10.1080/15325000903273403.
[9] K. Bhumkittipich and W. Phuangpornpitak, "Optimal placement and sizing of distributed generation for power loss reduction using particle swarm optimization," *Energy Proc.*, vol. 34, pp. 307–317, Jan. 2013, doi: 10.1016/j.egypro.2013.06.759.
[10] R. Kollu, S. R. Rayapudi, and V. L. N. Sadhu, "A novel method for optimal placement of distributed generation in distribution systems using HSDO," *Int. Trans. Electr. Energy Syst.*, vol. 24, no. 4, pp. 547–561, Apr. 2014, doi: 10.1002/etep.1710.
[11] S. A. Daud, A. F. Abdul Kadir, C. K. Gan, A. R. Abdullah, M. F. Sulaima, and N. H. Shamsudin, "Optimal placement and sizing of renewable distributed generation via gravitational search algorithm," in *Applied Mechanics and Materials*, vol. 785. Freienbach, Switzerland: Trans Tech Publications Ltd, 2015, pp. 556–560, doi: 10.4028/www.scientific.net/AMM.785.556.
[12] Z. Ullah, M. R. Elkadeem, S. Wang, and S. M. A. Akber, "Optimal planning of RDS considering PV uncertainty with different load models using artificial intelligence techniques," *Int. J. Web Grid Services*, vol. 16, no. 1, pp. 63–80, 2020, doi: 10.1504/IJWGS.2020.106126.
[13] N. Hantash, T. Khatib, and M. Khammash, "An improved particle swarm optimization algorithm forOptimal allocation of distributed generation units in radial power systems," *Appl. Comput. Intell. Soft Comput.*, vol. 2020, pp. 1–8, Sep. 2020, doi: 10.1155/2020/8824988.
[14] A. Waqar, U. Subramaniam, K. Farzana, R. M. Elavarasan, H. U. R. Habib, M. Zahid, and E. Hossain, "Analysis of optimal deployment of several DGs in distribution networks using plant propagation algorithm," *IEEE Access*, vol. 8, pp. 175546–175562, 2020, doi: 10.1109/ACCESS.2020.3025782.
[15] K. Dharageshwari and C. Nayanatara, "Multiobjective optimal placement of multiple distributed generations in IEEE 33 bus radial system using simulated annealing," in *Proc. Int. Conf. Circuits, Power Comput. Technol. ICCPCT*, Mar. 2015, pp. 1–7, doi: 10.1109/ICCPCT.2015.7159428.
[16] S. K. Sudabattula and M. Kowsalya, "Optimal allocation of solar based distributed generators in distribution system using bat algorithm," *Perspect. Sci.*, vol. 8, pp. 270–272, Sep. 2016, doi: 10.1016/j.pisc.2016.04.048.
[17] T. P. Nguyen, T. T. Tran, and D. N. Vo, "Improved stochastic fractal search algorithm with chaos for optimal determination of location, size, and quantity of distributed generators in distribution systems," *Neural Comput. Appl.*, vol. 31, no. 11, pp. 7707–7732, Nov. 2019, doi: 10.1007/s00521-018-3603-1.
[18] K. Balu and V. Mukherjee, "Optimal siting and sizing of distributed generation in radial distribution system using a novel student psychology-based optimization algorithm," *Neural Comput. Appl.*, vol. 33, pp. 15639–15667, Jun. 2021, doi: 10.1007/s00521-021-06185-2.
[19] R. Viral and D. K. Khatod, "An analytical approach for sizing and siting of DGs in balanced radial distribution networks for loss minimization," *Int. J. Electr. Power Energy Syst.*, vol. 67, pp. 191–201, May 2015, doi: 10.1016/j.ijepes.2014.11.017.
[20] M. M. Aman, G. B. Jasmon, A. H. A. Bakar, and H. Mokhlis, "A new approach for optimum simultaneous multi-DG distributed generation units placement and sizing based on maximization of system loadability using HPSO (hybrid particle swarm optimization) algorithm," *Energy*, vol. 66, no. 4, pp. 202–215, 2014, doi: 10.1016/j.energy.2013.12.037.
[21] A. Fathy, D. Yousri, A. Y. Abdelaziz, and H. S. Ramadan, "Robust approach based chimp optimization algorithm for minimizing power loss of electrical distribution networks via allocating distributed generators," *Sustain. Energy Technol. Assessments*, vol. 47, Oct. 2021, Art. no. 101359, doi: 10.1016/j.seta.2021.101359.
[22] A. Ali, M. U. Keerio, and J. A. Laghari, "Optimal site and size of distributed generation allocation in radial distribution network using multiobjective optimization," *J. Mod. Power Syst. Clean Energy*, vol. 9, no. 2, pp. 404–415, 2021, doi: 10.35833/MPCE.2019.000055.
[23] M. Azam Muhammad, H. Mokhlis, K. Naidu, A. Amin, J. Fredy Franco, and M. Othman, "Distribution network planning enhancement via network reconfiguration and DG integration using dataset approach and water cycle algorithm," *J. Mod. Power Syst. Clean Energy*, vol. 8, no. 1, pp. 86–93, 2020, doi: 10.35833/MPCE.2018.000503.
[24] E. S. Ali, S. M. Abd Elazim, and A. Y. Abdelaziz, "Ant lion optimization algorithm for optimal location and sizing of renewable distributed generations," *Renew. Energy*, vol. 101, pp. 1311–1324, Feb. 2017, doi: 10.1016/j.renene.2016.09.023.
[25] A. Ahmed, M. F. N. Khan, I. Khan, H. Alquhayz, M. A. Khan, and A. T. Kiani, "A novel framework to determine the impact of time varying load models on wind DG planning," *IEEE Access*, vol. 9, pp. 11342–11357, 2021, doi: 10.1109/ACCESS.2021.3050307.
[26] I. S. R. Khenissi, M. A. Fakhfakh, and R. Neji, "Power loss minimization using optimal placement and sizing of photovoltaic distributed generation under daily load consumption profile with PSO and GA algorithms," *J. Control, Automat. Elect. Syst.*, vol. 32, pp. 1317–1331, Jun. 2021, doi: 10.1007/s40313-021-00744-7.
[27] E. C. da Silva, O. D. Melgar-Dominguez, and R. Romero, "Simultaneous distributed generation and electric vehicles hosting capacity assessment in electric distribution systems," *IEEE Access*, vol. 9, pp. 110927–110939, 2021, doi: 10.1109/ACCESS.2021.3102684.
[28] T. P. Nguyen, T. A. Nguyen, T. V.-H. Phan, and D. N. Vo, "A comprehensive analysis for multi-objective distributed generations and capacitor banks placement in radial distribution networks using hybrid neural network algorithm," *Knowl.-Based Syst.*, vol. 231, Nov. 2021, Art. no. 107387, doi: 10.1016/j.knosys.2021.107387.
[29] M. Khasanov, S. Kamel, C. Rahmann, H. M. Hasanien, and A. Al-Durra, "Optimal distributed generation and battery energy storage units integration in distribution systems considering power generation uncertainty," *IET Gener., Transmiss. Distrib.*, vol. 15, no. 24, pp. 3400–3422, Dec. 2021, doi: 10.1049/gtd2.12230.
[30] N. Dharavat, S. K. Sudabattula, and S. Velamuri, "Optimal allocation of multiple distributed generators and shunt capacitors in a distribution system using political optimization algorithm," *Int. J. Renew. Energy Res.*, vol. 11, no. 4, pp. 1478–1488, 2021, doi: 10.20508/ijrer.v11i4.12240.g8349.
[31] S. Arulprakasam and S. Muthusamy, "Modified rainfall optimization based method for solving distributed generation placement and reconfiguration problems in distribution networks," *Int. J. Numer. Model., Electron. Netw., Devices Fields*, Nov. 2021, doi: 10.1002/jnm.2977.
[32] A. Shaheen, A. Elsayed, A. Ginidi, R. El-Sehiemy, and E. Elattar, "Reconfiguration of electrical distribution network-based DG and capacitors allocations using artificial ecosystem optimizer: Practical case study," *Alexandria Eng. J.*, vol. 61, no. 8, pp. 6105–6118, Aug. 2022, doi: 10.1016/j.aej.2021.11.035.
[33] S. Velamuri, S. H. C. Cherukuri, S. K. Sudabattula, N. Prabaharan, and E. Hossain, "Combined approach for power loss minimization in distribution networks in the presence of gridable electric vehicles and dispersed generation," *IEEE Syst. J.*, early access, Nov. 22, 2021, doi: 10.1109/JSYST.2021.3123436.
[34] M. Purlu and B. E. Turkay, "Estimating the distributed generation unit sizing and its effects on the distribution system by using machine learning methods," *Elektronika ir Elektrotechnika*, vol. 27, no. 4, pp. 24–32, Aug. 2021, doi: 10.5755/j02.eie.28864.
[35] A. D. Le, M. A. Kashem, M. Negnevitsky, and G. Ledwich, "Minimising voltage deviation in distribution feeders by optimising size and location of distributed generation," *Austral. J. Electr. Electron. Eng.*, vol. 3, no. 2, pp. 147–155, Jan. 2007, doi: 10.1080/1448837X.2007.11464155.
[36] Z. Ullah, M. R. Elkadeem, S. Wang, S. W. Sharshir, and M. Azam, "Planning optimization and stochastic analysis of RE-DGs for techno-economic benefit maximization in distribution networks," *Internet Things*, vol. 11, Sep. 2020, Art. no. 100210, doi: 10.1016/j.iot.2020.100210.
[37] Z. Ullah, M. R. Elkadeem, S. Wang, S. W. Sharshir, and M. Azam, "Planning optimization and stochastic analysis of RE-DGs for techno-economic benefit maximization in distribution networks," *Internet Things*, vol. 11, Sep. 2020, Art. no. 100210, doi: 10.1016/j.iot.2020.100210.
[38] M. H. Ali, S. Kamel, M. H. Hassan, M. Tostado-Véliz, and H. M. Zawbaa, "An improved wild horse optimization algorithm for reliability based optimal DG planning of radial distribution networks," *Energy Rep.*, vol. 8, pp. 582–604, Nov. 2022, doi: 10.1016/j.egyr.2021.12.023.
[39] T. T. Nguyen, T. T. Nguyen, and M. Q. Duong, "An improved equilibrium optimizer for optimal placement of photovoltaic systems in radial distribution power networks," *Neural Comput. Appl.*, Jan. 2022. [Online]. Available: https://link.springer.com/journal/521/online-first?page=5, doi: 10.1007/s00521-021-06779-w.
[40] *Metaheuristic*. Accessed: Dec. 1, 2021. [Online]. Available: https://en.wikipedia.org/wiki/Metaheuristic

[41] J. H. Holland, *Adaptation in Natural and Artificial Systems*, 1st ed. Cambridge, MA, USA: MIT Press, 1975.
[42] D. E. Goldberg, *Genetic Algorithms in Search, Optimization, and Machine Learning*. Reading, MA, USA: Addison-Wesley, 1989.
[43] J. Xiong, X. Liu, X. Zhu, H. Zhu, H. Li, and Q. Zhang, "Semi-supervised fuzzy C-means clustering optimized by simulated annealing and genetic algorithm for fault diagnosis of bearings," *IEEE Access*, vol. 8, pp. 181976–181987, 2020, doi: 10.1109/ACCESS.2020.3021720.
[44] A. Jafari, T. Khalili, E. Babaei, and A. Bidram, "A hybrid optimization technique using exchange market and genetic algorithms," *IEEE Access*, vol. 8, pp. 2417–2427, 2020, doi: 10.1109/ACCESS.2019.2962153.
[45] G. V. N. Lakshmi, A. Jayalaxmi, and V. Veeramsetty, "Optimal placement of distribution generation in radial distribution system using hybrid genetic dragonfly algorithm," *Technol. Econ. Smart Grids Sustain. Energy*, vol. 6, no. 1, pp. 1–13, Dec. 2021, doi: 10.1007/s40866-021-00107-w.
[46] S. A. G. Shirazi and M. B. Menhaj, "A new genetic based algorithm for channel assignment problems," in *Computational Intelligence, Theory and Applications*. Berlin, Germany: Springer, 2006, pp. 85–91, doi: 10.1007/3-540-34783-6_10.
[47] D. T. Viet, V. V. Phuong, M. Q. Duong, and Q. T. Tran, "Models for short-term wind power forecasting based on improved artificial neural network using particle swarm optimization and genetic algorithms," *Energies*, vol. 13, no. 11, p. 2873, Jun. 2020, doi: 10.3390/en13112873.
[48] J. T. Gao, C. H. Shih, C. W. Lee, and K. Y. Lo, "An active and reactive power controller for battery energy storage system in microgrids," *IEEE Access*, vol. 10, pp. 10490–10499, 2022, doi: 10.1109/ACCESS.2022.3145009.
[49] J. Kennedy and R. Eberhart, "Particle swarm optimization," in *Proc. 4th Int. Conf. Neural Netw.*, Nov./Dec. 1995, pp. 1942–1948.
[50] N. C. Hien, N. Mithulananthan, and R. C. Bansal, "Location and sizing of distributed generation units for loadabilty enhancement in primary feeder," *IEEE Syst. J.*, vol. 7, no. 4, pp. 797–806, Dec. 2013, doi: 10.1109/JSYST.2012.2234396.
[51] R. E. Perez and K. Behdinan, "Particle swarm optimization in structural design," in *Swarm Intelligence: Focus on Ant and Particle Swarm Optimization*, vol. 532. Rijeka, Croatia: InTech, 2007.
[52] F. A. Jumaa, O. M. Neda, and M. A. Mhawesh, "Optimal distributed generation placement using artificial intelligence for improving active radial distribution system," *Bull. Electr. Eng. Informat.*, vol. 10, no. 5, pp. 2345–2354, Oct. 2021, doi: 10.11591/eei.v10i5.2949.
[53] K. Gopalakrishnan, "Neural network–swarm intelligence hybrid nonlinear optimization algorithm for pavement moduli back-calculation," *J. Transp. Eng.*, vol. 136, no. 6, pp. 528–536, 2010, doi: 10.1061/(ASCE)TE.1943-5436.0000128.
[54] M. Zubair and M. Moinuddin, "Joint optimization of microstrip patch antennas using particle swarm optimization for UWB systems," *Int. J. Antennas Propag.*, vol. 2013, pp. 1–8, 2013, doi: 10.1155/2013/649049.
[55] E. Aydin, M. Purlu, and B. E. Turkay, "Economic dispatch of multi-microgrid systems by using particle swarm optimization," in *Proc. 13th Int. Conf. Electr. Electron. Eng. (ELECO)*, Nov. 2021, pp. 268–272, doi: 10.23919/ELECO54474.2021.9677839.
[56] A. Kaya and A. Bozkurt, "Determining optimum location and sizing of distributed generation systems in a real radial distribution network," *Electrica*, vol. 21, no. 3, pp. 342–351, Sep. 2021, doi: 10.5152/electrica.2021.21038.
[57] S. Essallah, A. Bouallegue, and A. K. Khedher, "Optimal sizing and placement of DG units in radial distribution system," *Int. J. Renew. Energy Res.*, vol. 8, no. 1, pp. 166–177, 2018.
[58] E. M. Ahmed, S. Rakočević, M. Ćalasan, Z. M. Ali, H. M. Hasanien, R. A. Turky, and S. H. E. A. Aleem, "BONMIN solver-based coordination of distributed FACTS compensators and distributed generation units in modern distribution networks," *Ain Shams Eng. J.*, vol. 13, no. 4, Jun. 2022, Art. no. 101664, doi: 10.1016/j.asej.2021.101664.
[59] P. D. P. Reddy, V. C. V. Reddy, and T. G. Manohar, "Ant lion optimization algorithm for optimal sizing of renewable energy resources for loss reduction in distribution systems," *J. Electr. Syst. Inf. Technol.*, vol. 5, no. 3, pp. 663–680, Dec. 2018, doi: 10.1016/j.jesit.2017.06.001.
[60] J. Rudresha, S. G. Ankaliki, T. Ananthapadmanabha, and V. Girish, "Application of hybrid techniques for optimal position and sizing of distributed generation units in radial distribution system," *Int. J. Elect. Eng. Technol.*, vol. 12, no. 2, pp. 90–99, Feb. 2021.

MIKAIL PURLU was born in Sivas, Turkey. He received the B.S. degree in electrical and electronics engineering form Sivas Cumhuriyet University, Sivas, Turkey, in 2013, and the M.S. degree in electrical engineering from Istanbul Technical University (ITU), Istanbul, Turkey, in 2017, where he is currently pursuing the Ph.D. degree in electrical engineering.

Since 2015, he has been a Research Assistant at ITU. His research interests include distributed generation, optimization of power systems, renewable energy, and smart grids.

BELGIN EMRE TURKAY was born in Istanbul, Turkey. She received the B.S., M.S., and Ph.D. degrees in electrical engineering from Istanbul Technical University (ITU), Istanbul.

She is currently a Professor and the Head of the Department of Electrical Engineering, ITU. Her research interests include power quality, renewable energy, and smart grids. She is a member of CIGRE Turkey and an Editor of the *Turkish Journal of Electrical Power and Energy Systems* (TEPES).